Stock assessment of blue marlin (*Makaira nigricans*) in the Indian Ocean using Stock Synthesis

Wen-Qi Xu, Chih-Yu Lin, Sheng-Ping Wang*

Department of Environmental Biology and Fisheries Science, National Taiwan Ocean University, Keelung, Taiwan.
* Corresponding author: wsp@mail.ntou.edu.tw

ABSTRACT

In this study, Stock Synthesis (SS) was applied to evaluate the stock status of blue marlin (*Makaira nigricans*) in the Indian Ocean, using a combination of historical catch records, standardized CPUE indices, and length-frequency data. Notably, compared with the previous assessment conducted in 2022, the recent upward trends in CPUE observed for most fleets have contributed to a more optimistic perception of the current stock status. While the SS model provides a comprehensive framework for integrating available data, the resulting management advice should be interpreted with caution and viewed in the context of these underlying uncertainties. The assessment results demonstrated that estimates of current stock status were influenced by model assumptions, particularly those related to natural mortality and stock-recruitment steepness. Furthermore, most life-history parameters used in this assessment were derived from studies of blue marlin in the Pacific Ocean, and this reliance on external parameter values introduces additional uncertainty into the evaluation of stock status in the Indian Ocean.

1. INTRODUCTION

The stock status of blue marlin (*Makaira nigricans*) in the Indian Ocean was evaluated based on the results of the 2022 benchmark assessment, which applied both the Bayesian state-space biomass production model JABBA and the integrated age-structured model Stock Synthesis (SS). Both models produced consistent results, indicating that the stock was overfished ($B_{2020}/B_{MSY} = 0.73$) and subject to overfishing ($F_{2020}/F_{MSY} = 1.13$). According to the weight of evidence, the stock was placed in the red quadrant of the Kobe plot, with an estimated 72% probability of being subject to overfishing and overfished (IOTC, 2022; 2024).

The biomass trajectory (B/B_{MSY}) has shown a long-term declining trend since the mid-1980s. A temporary increase occurred between 2007 and 2012, which coincided with the period of reduced fishing activity in the northwestern Indian Ocean due to piracy, after which the biomass declined again in recent years. Fishing mortality (F/F_{MSY}) has remained above 1 since the mid-1980s, despite some short-term fluctuations.

Based on this evidence, the stock is currently considered to be both overfished and subject to overfishing. Average catches from 2019 to 2023 (7,049 t) were lower than the estimated MSY (8,740 t), although the probability of rebuilding depends on further catch reductions.

Because historical standardized CPUE and length-frequency data are available for blue marlin in the Indian Ocean, and because auxiliary biological information (such as life-history parameters) can be obtained from previous stock assessments conducted for blue marlin in other oceans, the integrated stock assessment approach is appropriate for evaluating the stock status of blue marlin in the Indian Ocean. Accordingly, the present study undertakes a new stock assessment for blue marlin in the Indian Ocean using Stock Synthesis (SS; Methot, 2012; Methot and Wetzel, 2013).

2. MATERIALS AND METHODS

2.1 Fishery definition

Blue marlin in the Indian Ocean has been primarily exploited by longline fleets operated by Taiwan, Japan, and Indonesia, as well as by gillnet fleets from Pakistan, Iran, and Sri Lanka. However, catch data and standardized CPUE series were available only for the Taiwanese, Japanese, and Indonesian longline fleets. With respect to length-frequency data, long-term records exist only for the Taiwanese and Japanese fleets, although data have also become available in recent years for some other fleets. Nevertheless, the sample sizes for these additional fleets were sparse in most years.

In previous assessments, the fleets operating in the Indian Ocean were aggregated into four fisheries, including Japanese longline (JPN), Taiwanese longline (TWN), Indonesian longline (IDN), and other fleets (OTH). However, previous meetings have suggested that both relative abundance indices and size compositions may vary by area. In the present study, a two-area definition—west and east—was applied, following the area boundaries used for nominal catch by the Indian Ocean Tuna Commission (IOTC). This approach was used to separate Japanese, Taiwanese, and other fleets by area. As a result, the final fisheries configuration used in this assessment consisted of seven groups: JPN_W, JPN_E, TWN_W, TWN_E, IDN, OTH_W, and OTH_E.

2.2 Data used

Historical catch weights and length-frequency data for all fleets were provided by the Indian Ocean Tuna Commission (IOTC). Fig. 1 illustrates the trends in catch for the four fisheries considered in this study. Total catch increased markedly beginning in the early 1990s, with the majority of this increase attributed to the OTH and TWN fisheries.

The relative abundance indices used in this assessment were derived from the standardized CPUE of Taiwanese, Japanese, and Indonesian longline fleets (Xu et al., 2025; Kai, 2025; Setyadji et al., 2025). In addition, the standardized CPUE for the Taiwanese fleet was calculated by area and by CPUE standardization method, as shown in Fig. 2. Accordingly, the assessment models incorporated different combinations of these standardized CPUE series. Based on recommendations from the Working Party on Tropical Tunas (WPTT; IOTC, 2021), Taiwanese data prior to 2005 were not used for CPUE standardization due to concerns regarding data quality and the identification of fishing operations targeting tropical tunas. As a result, updated Taiwanese standardized CPUE data were available only from 2005 to 2023. Japanese standardized CPUE data were divided into two periods, with data from 1979 to 2010 (JPN_HIST) and from 2011 to 2023 (JPN), reflecting the contraction of operational areas for the Japanese longline fleet after 2010. Indonesian standardized CPUE data were available from 2006 to 2023.

Length data for blue marlin in the Indian Ocean were primarily collected by Japanese and Taiwanese longline fleets. Although some length data were also collected by other fleets, including those from Korea, Sri Lanka, European Union member countries, and China, the available time series from these sources were generally short or incomplete. All length-frequency data were converted to eye fork length (EFL) measurements and aggregated into 3 cm intervals, as shown in Fig. 3.

Fig. 4 presents the temporal coverage of available data for each fleet used in the stock assessment of blue marlin in the Indian Ocean, including catch, length-frequency, and CPUE data.

2.3. Life-history parameters

Because life-history parameters specific to blue marlin in the Indian Ocean are currently unavailable, the assessment models in this study utilized the same parameters adopted in the previous assessment (Xu, 2022). The values of all life-history parameters used in this study are listed in Table 1.

Blue marlin exhibit sexual dimorphism in growth, with females growing faster than males (Fig. 5; see also Lee et al., 2013, 2014). Stock Synthesis provides three growth models as options, including the von Bertalanffy growth curve, Schnute's

generalized growth curve (also known as the Richards curve), and the von Bertalanffy growth curve with age-specific deviations for the growth coefficient (K). In the present study, the standard von Bertalanffy growth curve was selected and parameterized as follows:

$$L_2 = L_\infty + (L_1 - L_\infty)e^{-K(A_2 - A_1)}$$

where L_1 and L_2 represent the lengths at the youngest (A_1) and oldest (A_2) ages observed in the data, K denotes the growth coefficient, and L_∞ is the theoretical maximum length, which can be calculated from the other three parameters. Growth parameters were fixed to those adopted by Lee et al. (2013, 2014) in their assessment of blue marlin in the Pacific Ocean.

Setyadji et al. (2014) provided a length-weight relationship for blue marlin in the Indian Ocean. However, applying this relationship resulted in unrealistically high weights for large fish when converting eye fork length (EFL) data. For this reason, the length-weight relationship developed by Lee et al. (2013, 2014) was adopted, consistent with the approach used in the previous assessment.

There is little information available on natural mortality (M) for blue marlin in the Indian Ocean. Lee et al. (2013, 2014) estimated sex- and age-specific natural mortality rates for blue marlin in the Pacific Ocean. Based on those estimates, age-specific natural mortality rates were fixed at 0.42 $year^{-1}$ for age 0, 0.37 $year^{-1}$ for age 1, 0.32 $year^{-1}$ for age 2, 0.27 $year^{-1}$ for age 3, and 0.22 $year^{-1}$ for age 4 and above for female. For males, natural mortality was set at 0.42 $year^{-1}$ for age 0, 0.37 $year^{-1}$ for age 1 and above. As the previous assessment, the values for adult fishes (0.22 $year^{-1}$ for females and 0.37 $year^{-1}$ for males) were used as a reference case for the assessment of blue marlin in the Indian Ocean. In addition, Lorenzo parameterization was also used to calculate age-specific natural mortality rates for females and males based on the growth and length-weight parameters (Fig. 6).

The maturity ogive for blue marlin in the western Pacific Ocean, as described by Sun et al. (2009), was used in this study. The length at 50% maturity was estimated to be 179.76 cm, and the slope of the logistic function was -0.2039.

The standard Beverton-Holt stock-recruitment relationship was applied in this study. Due to limited information regarding the steepness parameter (h), which represents stock productivity, the value adopted by Lee et al. (2013, 2014) was used, with h set at 0.87. To account for uncertainty in this parameter, sensitivity analyses were conducted using three alternative steepness values (h = 0.7, 0.8, and 0.95) in order to evaluate the robustness of the assessment results.

2.4 Model structure and assumption

Stock Synthesis (SS) version 3.30.22 (Methot et al., 2023) was used for all model runs in this study. Equal weighting was applied to all data components.

Although sex-specific data were not available, the model was constructed with a sex-specific population structure, allowing the age composition to be differentiated by sex within the population. The maximum age considered in the model was set at 40 years. The assessment period spanned from 1950 to 2023, with projections extending ten years into the future. The sex ratio for females was assumed to be 0.5.

Recruitment was estimated as deviations from the Beverton-Holt stock-recruitment relationship and was assumed to follow lognormally distributed deviates with a mean of zero and a standard deviation (σ_R). In this study, the value of σ_R was set at 0.4, which is commonly adopted in previous stock assessments for tunas and billfishes. Recruitment deviations were estimated for the years 1970 through 2023, and deviations for all other years were fixed at zero.

Selectivity curves were modeled as length-based double normal functions, as the length-frequency compositions for the fleets tended to be concentrated within specific ranges. Selectivity was assumed to be time-invariant for all fleets. Due to incomplete time series or insufficient sample sizes in the length-frequency data for the Indonesian (IDN) and Other (OTH) fleets, the selectivities for these fleets were assumed to be the same as those for the Taiwanese (TWN) fleet.

Catchability was estimated under the assumption that each survey index was proportional to the vulnerable biomass, with a scaling factor representing catchability. Catchability was assumed to be constant over time for all indices (Lee et al., 2013).

As recommended by Methot (2012), fishing mortality (F) was modeled using the hybrid F method. This approach applies Pope's approximation to provide initial values for the iterative adjustment of Baranov's continuous F values, thereby closely approximating the observed catch.

2.5 Diagnostics and retrospective analysis

Residual diagnostics for model fits and retrospective analyses were conducted using the functions available in the R package "ss3diags" (Carvalho et al., 2021). In addition, this package was used to implement a delta-multivariate lognormal approximation, which was applied to generate joint error distributions for both relative spawning biomass and fishing mortality in relation to the maximum sustainable yield (MSY) reference point.

2.6 Scenarios

The standardized CPUE series revealed different patterns across fleets and areas, although the trends were generally similar within each fleet (Fig. 2). To incorporate all

available information regarding relative abundance trends, the standardized CPUE series for the Taiwanese, Japanese, and Indonesian fleets were adopted for the assessment models. Models were then developed by incorporating various combinations of these standardized CPUE series, as summarized in Table 2.

Based on the life-history parameters, as well as the assumptions and structure of the model, a range of scenarios was constructed to examine how stock status estimates would respond to different input data and parameter values. The scenarios are summarized as follows:

S0: Same fleet data and model specification as scenario "S10" used in the previous assessment.

S1: Same model specification as S0, except that the Taiwanese CPUE data were replaced with CPUE series derived using sdmTMB.

S2: Same as S0, but with fixed natural mortality rates.

S3: Same as S1, but with fixed natural mortality rates.

S4~S6: Same as S0, but with alternative steepness values for the stock-recruitment relationship (h = 0.95, 0.8, and 0.7, respectively).

S7~S9: Same as S1, but with alternative steepness values (h = 0.95, 0.8, and 0.7, respectively).

3. RESULTS AND DISCUSSIONS

3.1. Model fits and diagnostics

Overall, SS models adequately captured the general trends in the standardized CPUE series for both the Taiwanese and Japanese fleets under all scenarios. Notably, the SS models effectively reflected the recent increases in CPUE that were observed across most fleets in the final years of the time series, particularly in 2023 (Fig. 7). This strong correspondence between the observed and model-predicted CPUE values in recent years indicates that the model is capable of incorporating and responding to the most updated information on relative abundance. The ability of the SS model to track the upward movement in CPUE indices in 2023 provides additional confidence that the assessment results are sensitive to recent changes in the underlying data.

The model fits to the length-frequency data and the associated Pearson residuals are presented in Figs. 3 and 8. Residual plots are shown for scenario S0 as an example, and similar patterns were observed across other scenarios. For the length-frequency data, the model fit was relatively poor for the Taiwanese fleet prior to the early 2000s. In these years, a greater proportion of small fish was present in the catch, and the model was unable to fully capture the observed distribution patterns (see Fig. 3, top left and

bottom left panels; Fig. 8, TWN_W and TWN_E). The model fit also deteriorated for the Japanese fleet after the early 2000s, primarily due to a reduced sample size and increased variability in the data (Fig. 3, top right and bottom right panels; Fig. 8, JPN_W and JPN_E).

However, the overall model fit to the length-frequency data should not be directly compared between the Taiwanese and Japanese fleets, given that most of the fish caught by the Japanese fleet were larger than 100 cm, resulting in an inherently different length composition. This difference is clearly reflected in the distributional patterns shown in Fig. 3.

The run test and joint residual plots obtained from all scenarios were shown in Figs. 9 and 10. Among all scenarios, S1, S3, S8, S7, and S9, which incorporated the sdmTMB-standardized CPUE indices for the Taiwanese fleet, yielded the lowest RMSE values among all scenarios for the CPUE fits, with values ranging from 21.3 to 22.2%. In contrast, scenarios that applied the delta-GLM-standardized CPUE series for Taiwan, including S0, S2, S4, S5, and S6, produced higher RMSE values, typically around 24.3 to 24.6%, as summarized in Fig. 9. Lower RMSE values generally indicate a more optimal agreement between the model and observed indices. However, it is essential to interpret these differences with care because the scenarios rely on different standardization methods for the Taiwanese CPUE. The sdmTMB method, which has been increasingly used in recent stock assessments, often generates a smoother and more stable abundance index, and this property can contribute to a closer match between model predictions and observed data. This methodological distinction should be considered when comparing RMSE values across scenarios.

For the fits to length-frequency data, RMSE values showed minimal variation across scenarios, remaining between 7.8 and 7.9% as shown in Fig. 10. This consistency indicates that the ability of the model to fit the observed size composition data is robust and relatively unaffected by the choice of CPUE index.

In summary, when selecting the most appropriate scenario for further inference, it is reasonable to consider both the quantitative metrics of fit, such as RMSE, and the suitability of the input data, especially regarding the CPUE standardization method. In this assessment, scenarios that used the sdmTMB-standardized Taiwanese CPUE, specifically S1, S3, S7, S8, and S9, can be regarded as providing more optimal fits to the observed CPUE series. Even so, this conclusion should be made with consideration of the methodological differences among CPUE standardization approaches and the overall quality of the available data.

3.2. Model estimates

The estimated selectivity curves for all scenarios, as shown in Fig. 11, consistently

indicate that the Taiwanese longline fleets (TWN_W and TWN_E) predominantly selected smaller blue marlin, with full selectivity attained at approximately 60 to 70 cm in length. In contrast, the Japanese fleets (JPN_W and JPN_E) exhibited broader selectivity patterns, targeting larger individuals and maintaining relatively high selectivity across a wider range of body sizes. The selectivity estimates were highly consistent among scenarios, demonstrating that the choice of input data or CPUE standardization method had minimal influence on the overall selectivity patterns for each fleet. These results reflect the inherent differences in fishing strategies and operational characteristics between the Taiwanese and Japanese longline fisheries.

The estimated time series of recruitment, spawning biomass, and fishing mortality under all scenarios are presented in Fig. 12. Recruitment exhibited a marked decline from the mid-1980s through 2000, which corresponded with a period of intensified fishing pressure and increased catches. The spawning biomass demonstrated a modest recovery from the late 2000s to the early 2010s. This rebound coincided with a period of elevated recruitment and a temporary reduction in fishing mortality. In recent years, however, both recruitment and spawning biomass have shown a persistent downward trend, which has occurred in conjunction with renewed increases in fishing mortality. These results highlight the dynamic relationship between fishing intensity, recruitment, and stock biomass in the blue marlin population of the Indian Ocean.

The time trajectories of relative spawning biomass and fishing mortality show broadly consistent patterns across all scenarios (Fig. 13). Spawning biomass, expressed as a proportion of the unfished level (SSB/SSB_0), declined steadily from approximately 1.0 in the 1950s to values between 0.1 and 0.4 in recent years. This pattern clearly indicates a substantial depletion of the stock over time. Similarly, the ratio of spawning biomass to the level that produces maximum sustainable yield (SSB/SSB_{MSY}) also exhibited a marked downward trend. Scenarios S4 and S7, which were based on a higher steepness value (h=0.95), maintained higher levels of SSB/SSB_{MSY}, remaining above 1.0 for a longer period relative to other scenarios. In contrast, most other scenarios showed recent SSB/SSB_{MSY} values near or below 1.0, which suggests diminished stock productivity in relation to sustainable reference points. During the same period, fishing mortality relative to F_{MSY} (F/F_{MSY}) increased sharply, rising from near zero in the early years to values that approached or exceeded 1.0 from the 2000s onward. Interannual variation in fishing mortality was particularly pronounced during the 2000s and 2010s. Collectively, these results indicate that the Indian Ocean blue marlin stock has undergone a significant decline in abundance and is currently experiencing elevated fishing pressure. Differences among scenarios primarily reflect the effects of varying model assumptions and input data.

The Kobe plot, which summarizes the estimated stock status across all scenarios

(Fig. 14), shows that most scenarios place the current blue marlin stock in the Indian Ocean within the quadrant representing neither overfished nor experiencing overfishing. While the majority of scenarios indicate that the stock status is above the limit reference points, the estimates are frequently near the threshold for being considered overfished. It is important to note that, under the assumption of low steepness (h=0.7), as represented by scenarios S6 and S9, the results suggest an increased risk that the stock may fall into the overfished and overfishing category. This outcome highlights the sensitivity of stock status conclusions to the assumed value of steepness and underscores the need for careful interpretation when making management recommendations.

In this study, scenario S1 was selected as the optimal scenario for management inference, as it retains the same model assumptions as the updated base case (S0) but utilizes the sdmTMB-standardized Taiwanese CPUE, which resulted in a noticeably lower RMSE for the CPUE fits. Although scenario S9 produced the lowest RMSE among all scenarios, its assumption of a low steepness parameter (h=0.7) is more suitable for sensitivity testing rather than for informing management advice. For this reason, scenario S1 offers a more reliable and internally consistent reference for evaluating the current stock status and for providing management recommendations. While the choice of CPUE standardization method can influence model fit, it is widely accepted practice to base the primary inference on the scenario that combines the most credible data with robust diagnostics under the main structural assumptions, rather than on a scenario defined primarily by a single sensitivity parameter.

The Kobe plots for scenarios S0 and S1 are presented in Figure 15. In both cases, the highest probability estimates indicate that the current stock status of blue marlin in the Indian Ocean is not overfished and not subject to overfishing, as most points are located in the green quadrant. However, scenario S1 shows a higher probability of the stock being classified as overfished or undergoing overfishing compared to S0, with the percentages rising to 4% for the overfished and overfishing quadrant and 30.6% for the overfished-only quadrant. These results highlight the sensitivity of stock status conclusions to the CPUE standardization method, particularly given the recent increases observed in the abundance indices.

Table 3 shows the model estimates of the key management quantities obtained from various scenarios. The estimates of current spawning biomass relative to unfished levels (SSB_{2023}/SSB_0) remain consistently low across all scenarios, indicating that this quantity is relatively robust to alternative model assumptions. In contrast, estimates of current spawning biomass and fishing mortality relative to their respective MSY reference points (SSB_{2023}/SSB_{MSY} and F_{2023}/F_{MSY}) show greater sensitivity, particularly to the steepness parameter and the CPUE standardization method used for the

Taiwanese fleet. Scenarios incorporating a lower steepness assumption produced more pessimistic estimates, suggesting a higher likelihood of the stock being overfished and subject to overfishing, whereas most other scenarios supported a more favorable stock status.

REFERENCE

Carvalho, F., Winker, H., Courtney, D., Kapur, M., Kell, L., Cardinale, M., Schirripag, M., Kitakado, T., Yemane, D., Piner, K.R., Maunder, M.N., Taylor, I., Wetzel, C.R., Doering, K., Johnsonm, K.F., Methot, R.D., 2021. A Cookbook for Using Model Diagnostics in Integrated Stock Assessments. Fish. Res. 240: 105959.

IOTC, 2021. Report of the 23rd Session of the IOTC Working Party on Tropical Tunas, Data Preparatory Meeting. IOTC-2021-WPTT23(DP)-R[E].

IOTC, 2024. Report of the 22nd Session of the IOTC Working Party on Billfish. IOTC-2024-WPB22-R[E].

Kai, M., 2025. Spatio-temporal model for CPUE standardization: application to blue marlin caught by Japanese tuna longline fishery in the Indian ocean from 1979 to 2023. IOTC-2025-WPB23-16.

Lee, H.H, Chang, Y.J, Hinton, M.G., Piner, K.R., Tagami, D., Taylor, I., Kai, M., 2013. Blue marlin (*Makaira nigricans*) stock assessment in the Pacific Ocean. ISC/13/BILLWG-2/04.

Lee, H.H., Piner, K.R., Methot Jr., R.D., Maunder, M.N., 2014. Use of likelihood profiling over a global scaling parameter to structure the population dynamics model: An example using blue marlin in the Pacific Ocean. Fish. Res. 158: 138-146.

Methot R.D., Wetzel, C.R., 2013. Stock synthesis: A biological and statistical framework for fish stock assessment and fishery management. Fish. Res. 142: 86-99.

Methot, R.D., 2012. User manual for Stock Synthesis. NOAA Fisheries, Seattle, WA.

Methot. R.D., Wetzel, C.R., Taylor, I.G., Doering, K.L., Gugliotti, E.F., Johnson, K.F., 2023. Stock Synthesis User Manual, version 3.30.22. NOAA Fisheries, Seattle, WA.

Parker, D., and Kerwath, S. 2022. Updated stock assessment of blue marlin (*Makaira nigricans*) in the Indian Ocean using JABBA. IOTC-2022-WPB20-12

Setyadji, B., Jatmiko, I., Wujdi, I., Nugraha, B., 2014. Preliminary analysis of length – weight relationship of swordfish (*Xiphias gladius*), black marlin (*Makaira indica*), and blue marlin (*Makaira nigricans*) caught by Indonesian longliners in the Indian Ocean. IOTC–2014–WPB12–13

Setyadji, B., Spencer, M., Kell, L., Wright, S., Ferson, S., 2025. Update on CPUE Standardization of Blue Marlin (*Makaira nigricans*) from Indonesian Tuna Longline Fleets 2006-2023. IOTC-2025-WPB23-15

Sun, C.L., Chang, Y.J., Tszeng, C.C., Yeh, S.Z., Su, N.J. 2009. Reproductive biology of blue marlin (*Makaira nigricans*) in the western Pacific Ocean. Fish. Bull. 107: 420-432.

Xu, W. Q., Wang, S. P., and Lin, C. Y. 2022. Stock assessment of blue marlin (*Makaira nigricans*) in the Indian Ocean using Stock Synthesis. IOTC-2022-WPB-13 rev1.

Xu, W.Q., Lin, C.Y., Wang, S.P., 2025. CPUE standardization of blue marlin (*Makaira nigricans*) caught by the Taiwanese large-scale longline fishery in the Indian Ocean using GLM and sdmTMB. IOTC-2025-WPB23-17.

Separate Japanese, Taiwanese and other fleets by areas

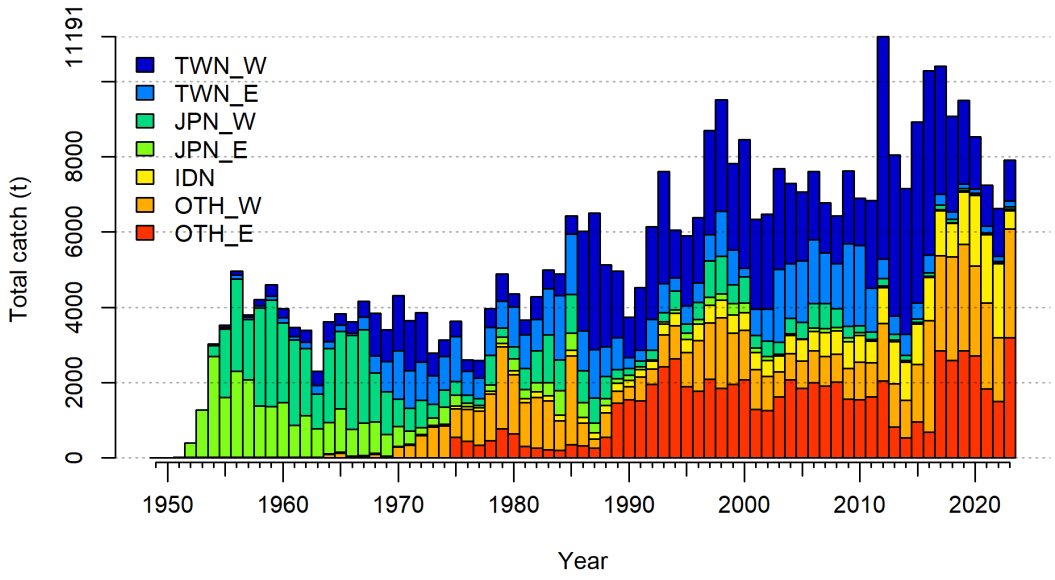

Fig. 1. Annual catches of blue marlin in the Indian Ocean by fleets.

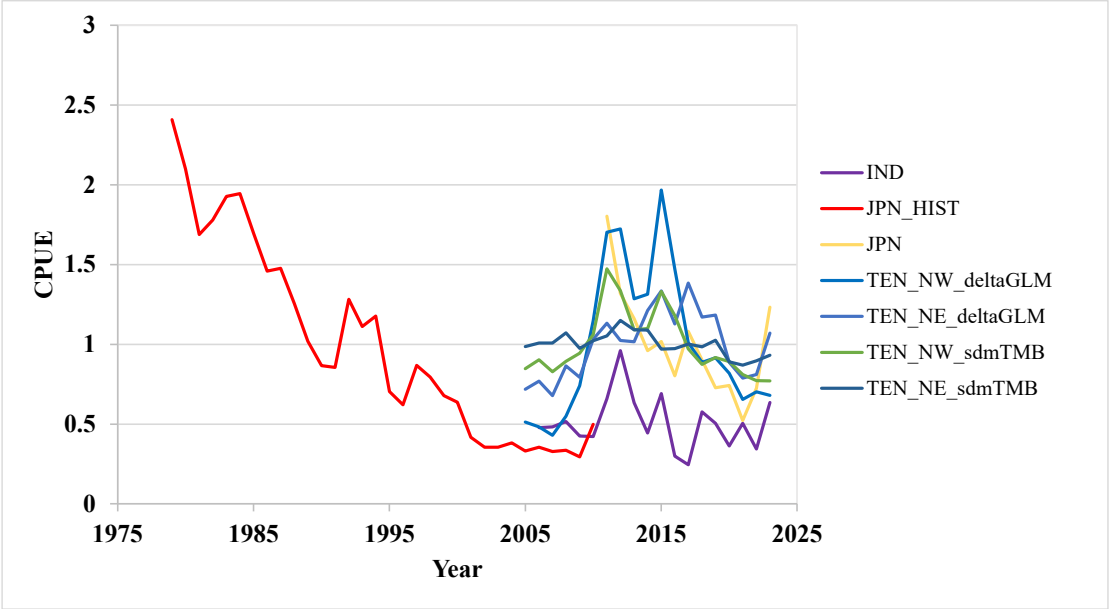

Fig. 2. Standardized CPUE series by fleets and areas used for the stock assessment of blue marlin in the Indian Ocean.

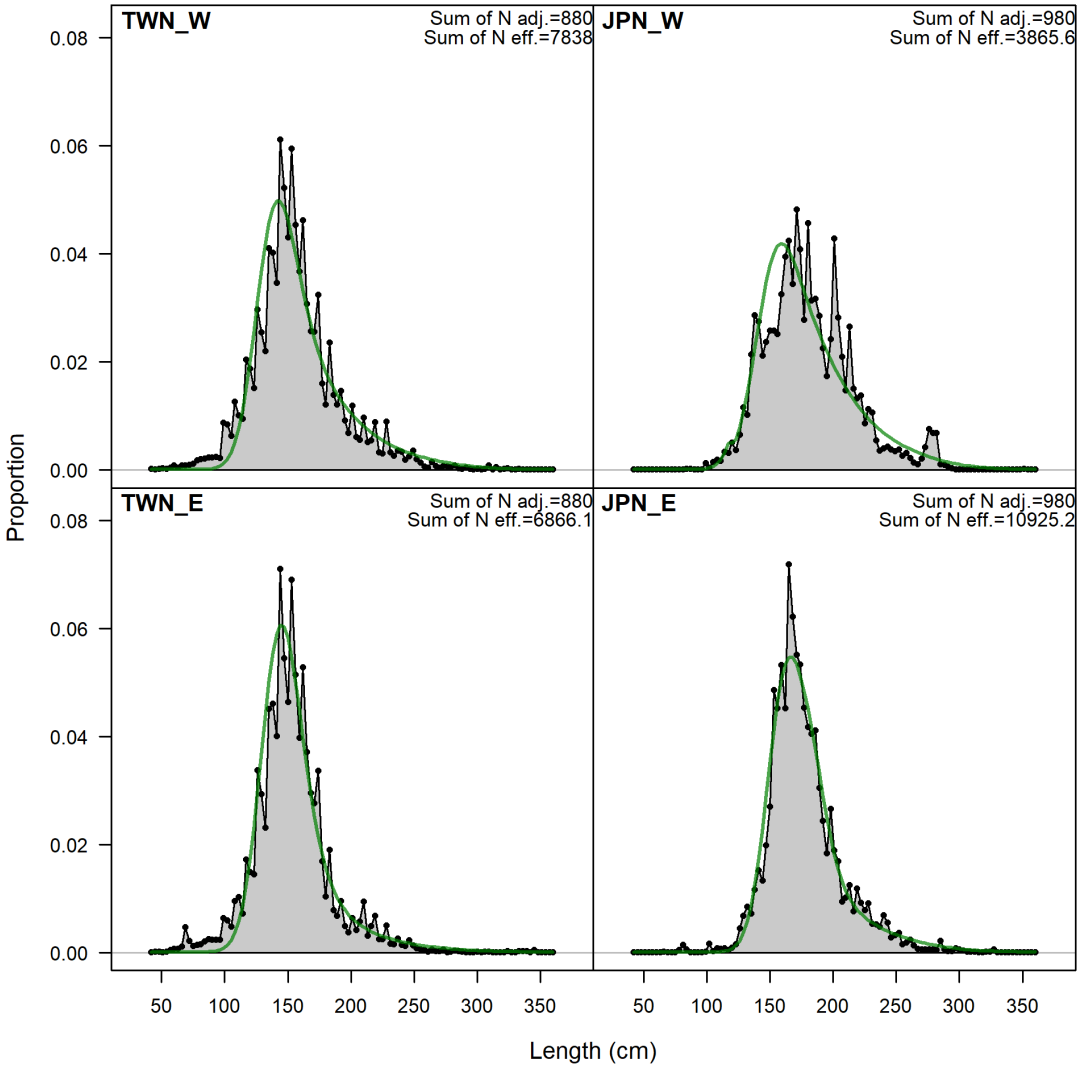

Fig. 3. Observed length-frequency aggregated across years of blue marlin in the Indian Ocean (predicted values were obtained from scenario “S0”).

S0

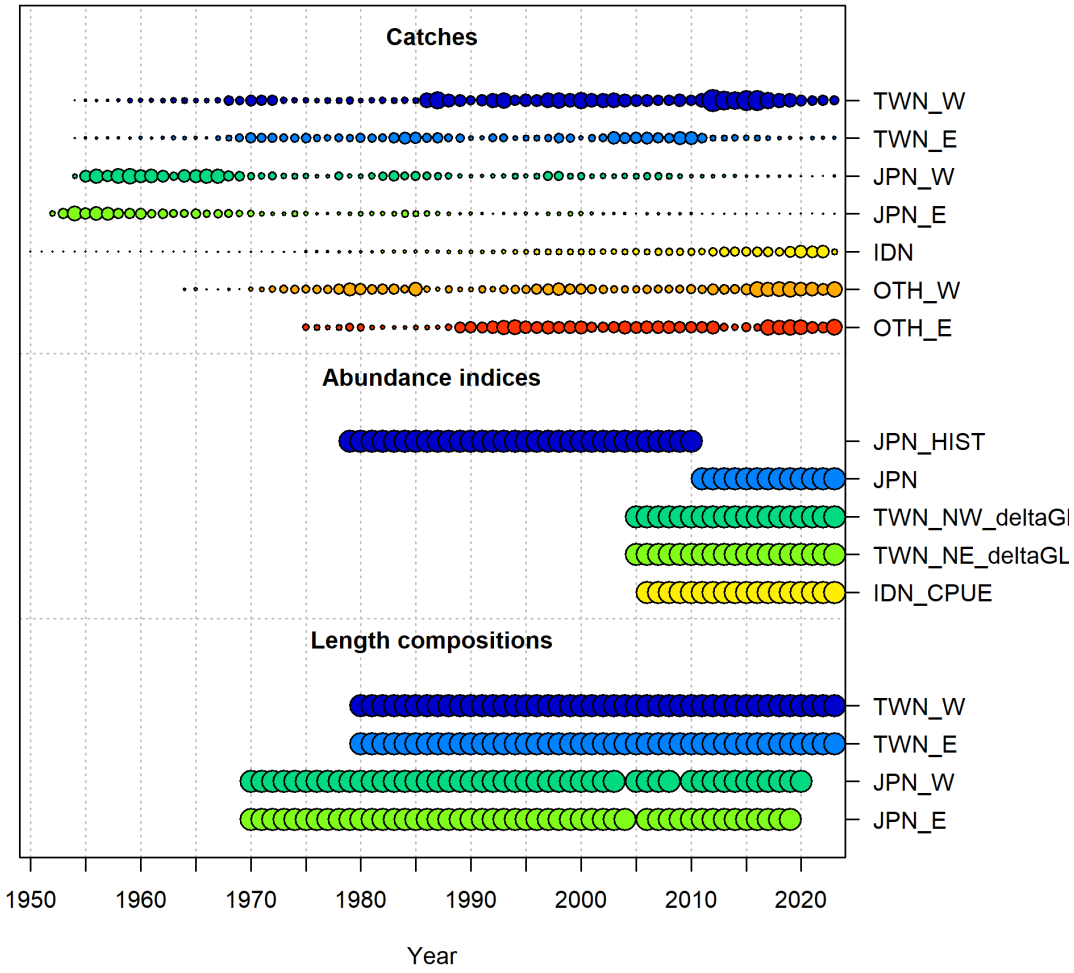

Fig. 4. Data presence by year for each fleet used for the stock assessment of blue marlin in the Indian Ocean.

S1

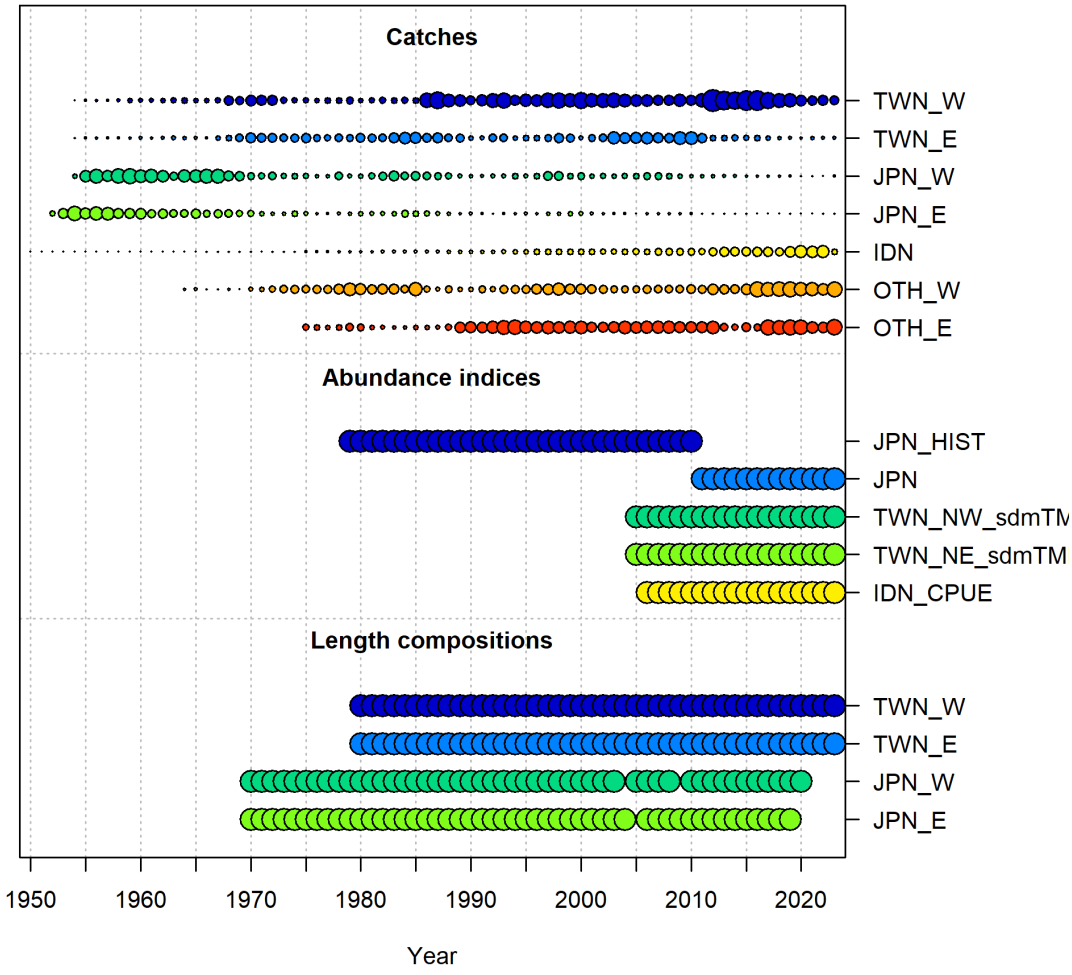

Fig. 4. (Continued).

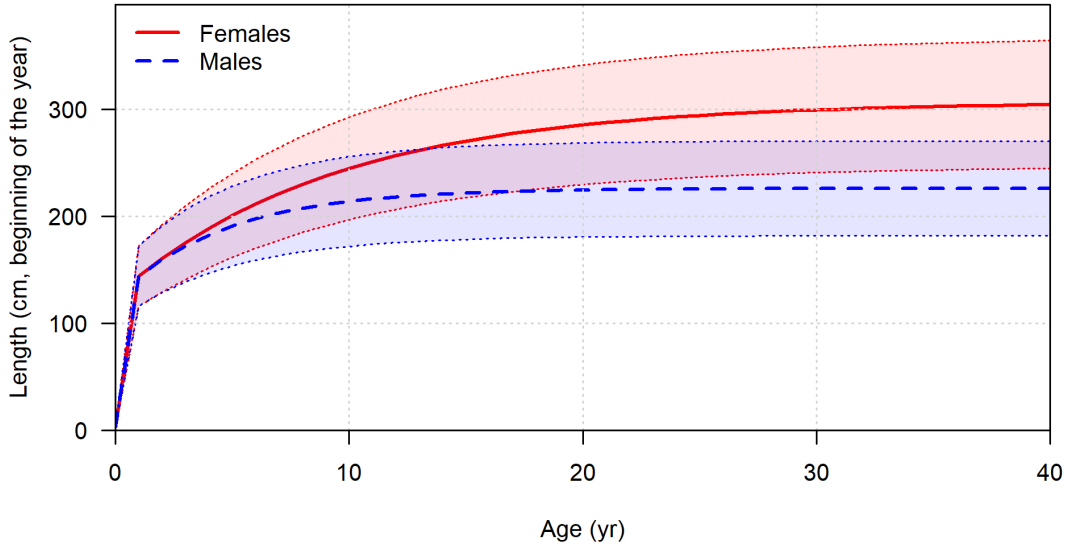

Fig. 5. Growth curves of blue marlin in the Indian Ocean.

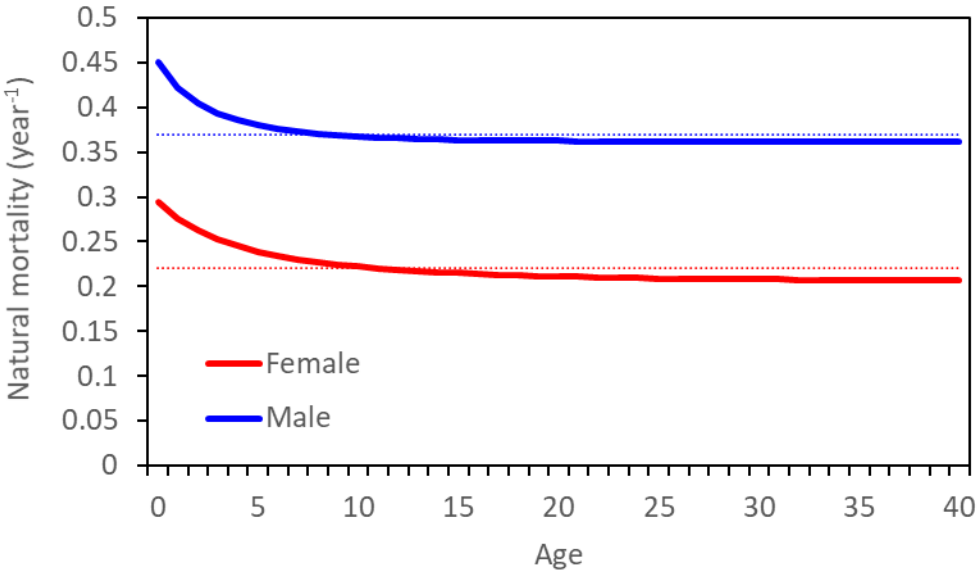

Fig. 6. The mean values of age-specific natural mortalities scaled to the same as fixed natural mortality.

TWN_NW_deltaGLM

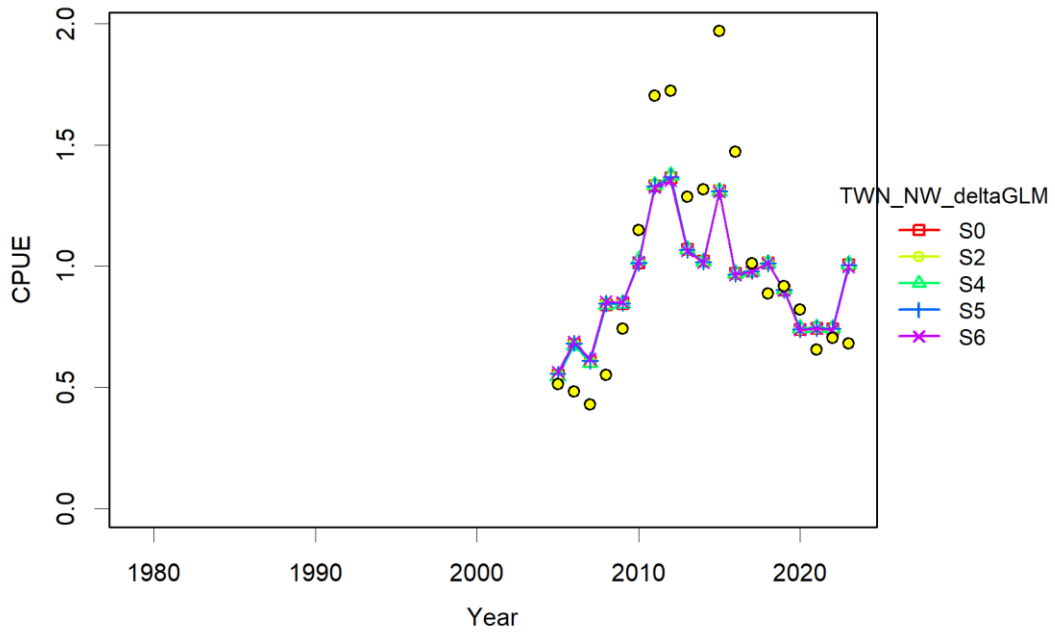

TWN_NE_deltaGLM

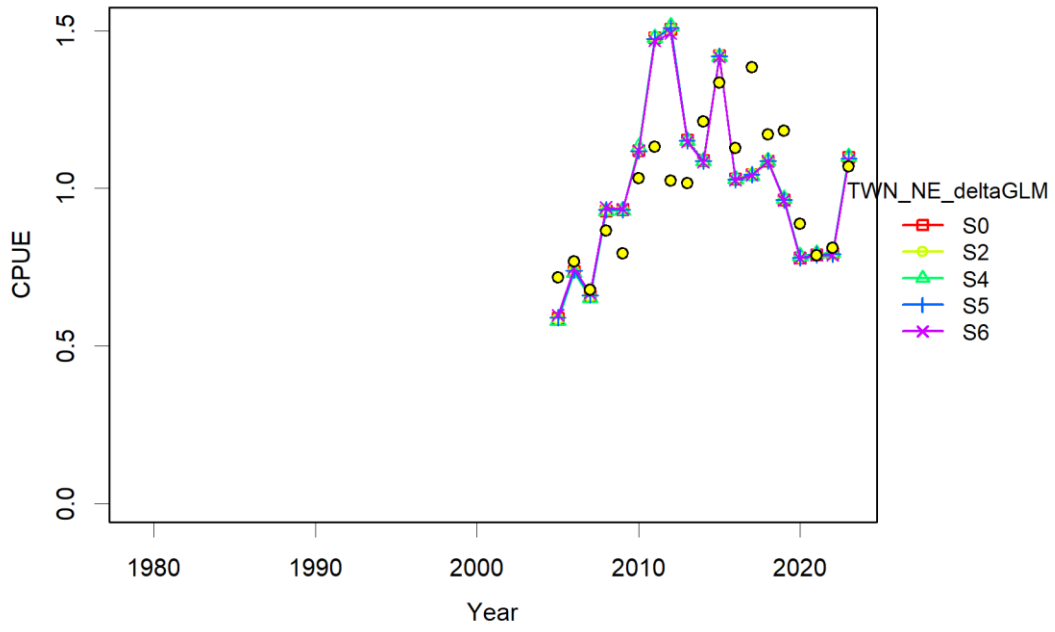

Fig. 7. Observed CPUE (dots) and model-estimated CPUE (lines) of blue marlin in the Indian Ocean.

TWN_NW_sdmTMB

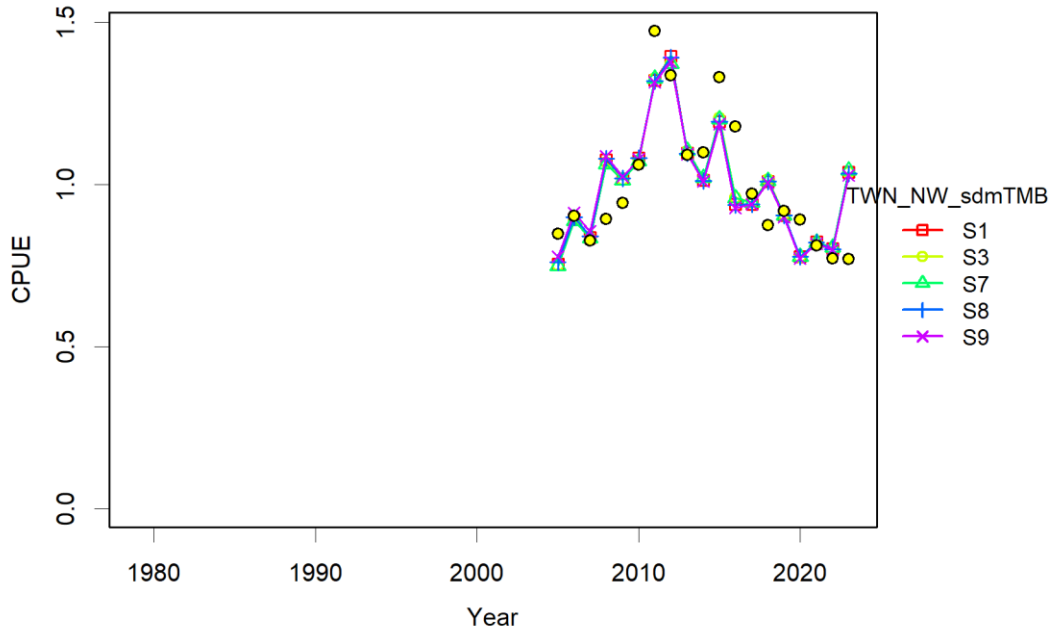

TWN_NE_ sdmTMB

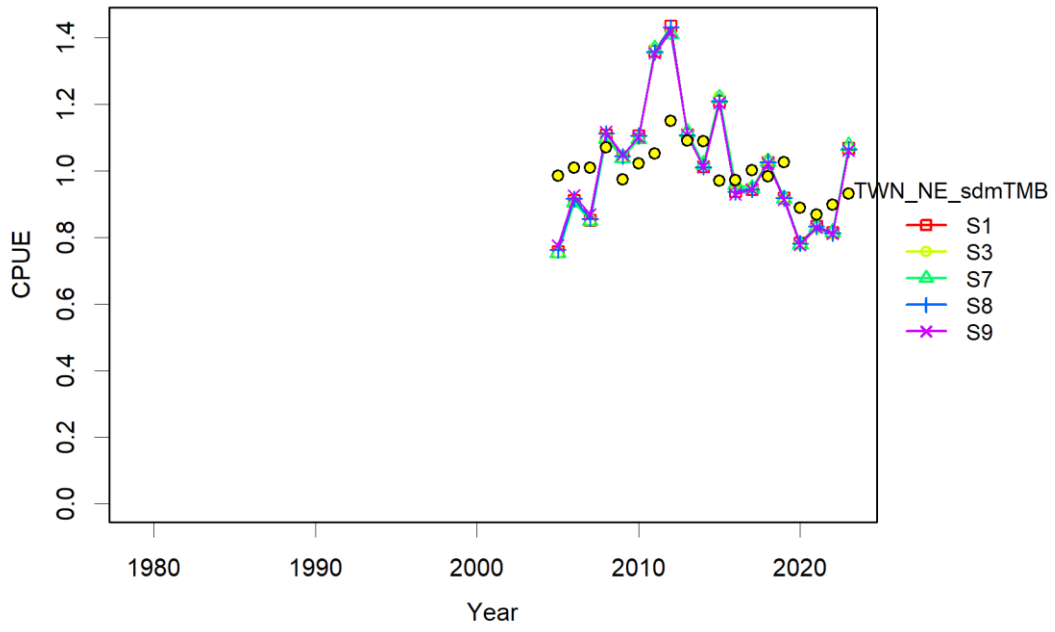

Fig. 7. (Continued).

JPN_HIST

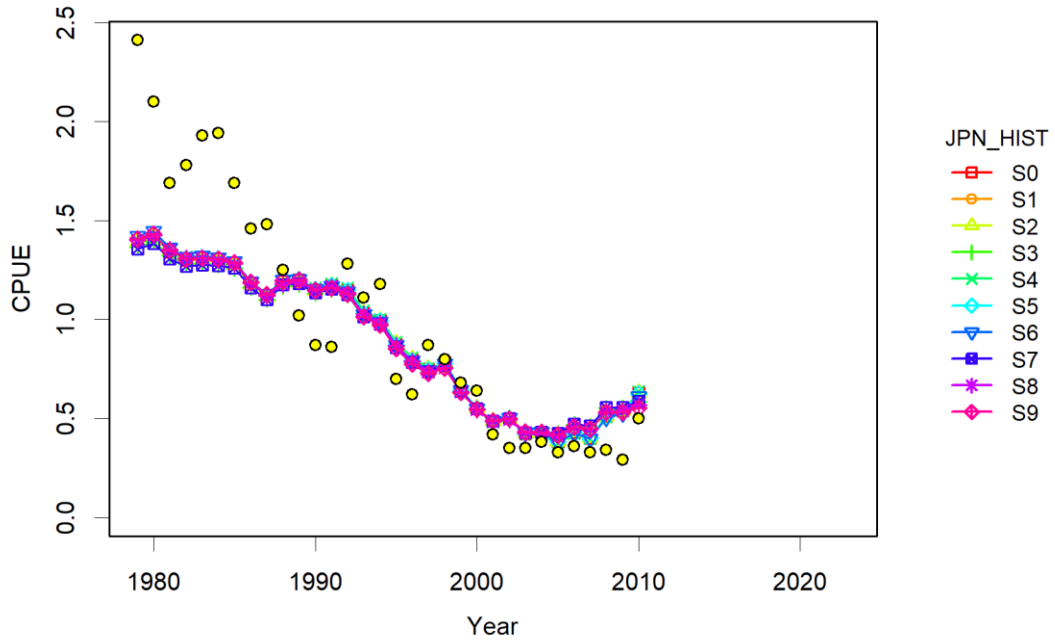

JPN

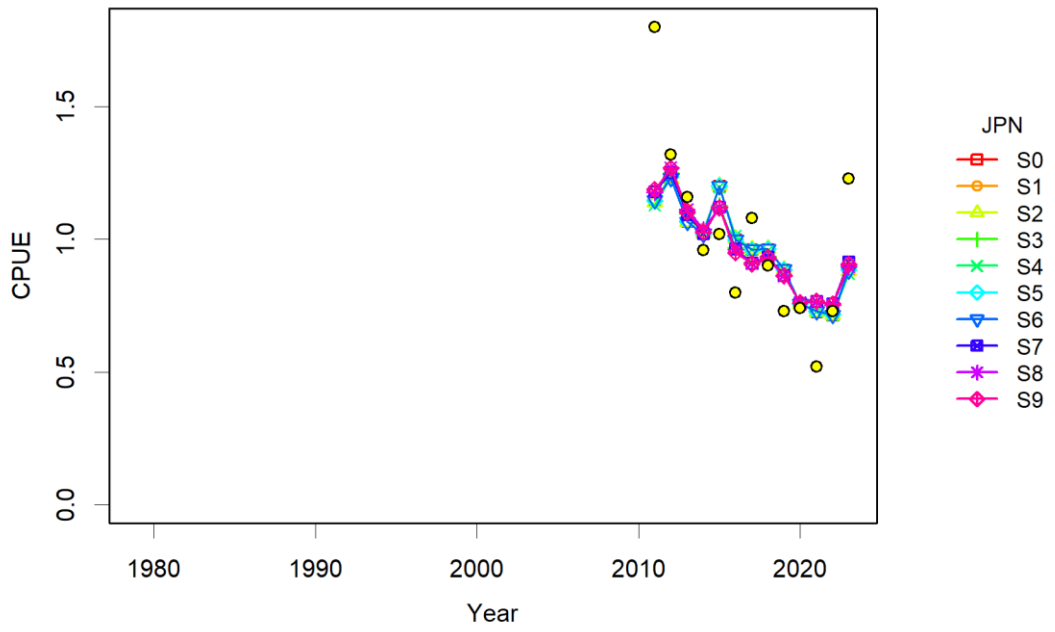

Fig. 7. (Continued).

IDN

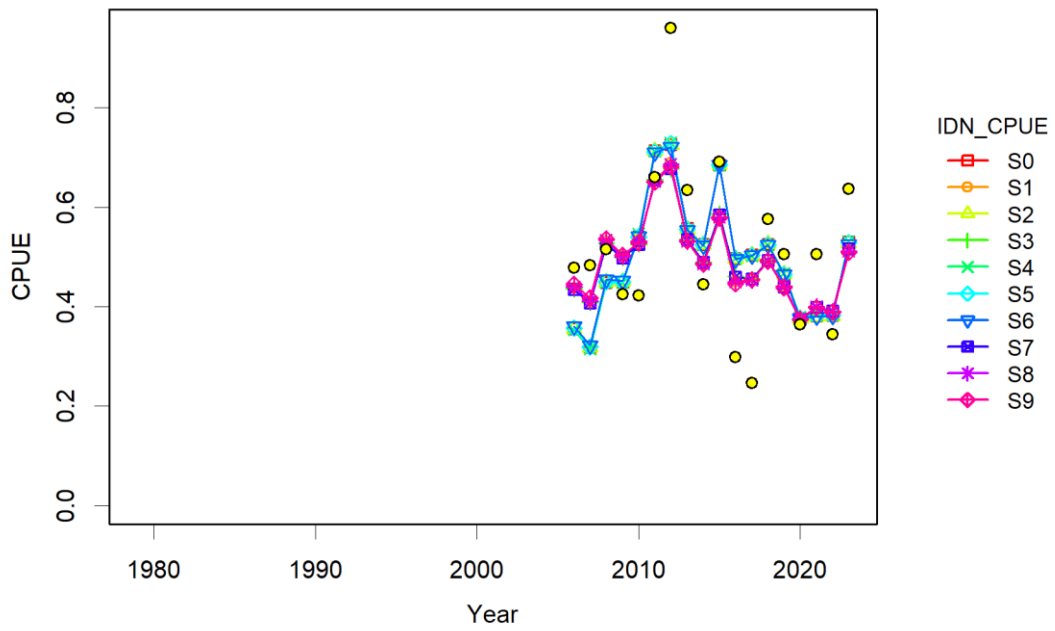

Fig. 7. (Continued).

Scenario “S0”

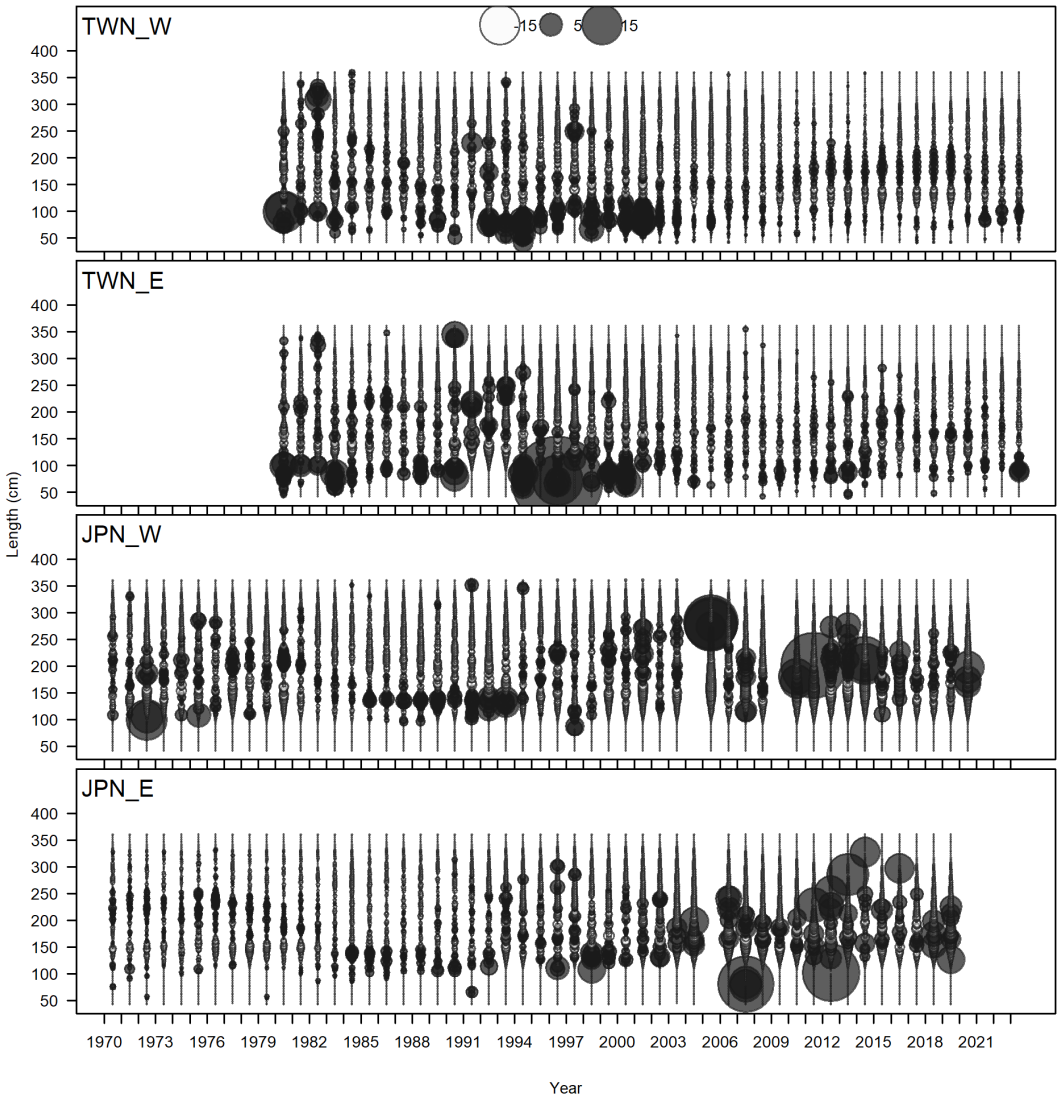

Fig. 8. Pearson residuals of the model fits to length-frequency data of blue marlin in the Indian Ocean. Closed bubbles are positive residuals (observed > expected) and open bubbles are negative residuals (observed < expected).

Scenario “S0”

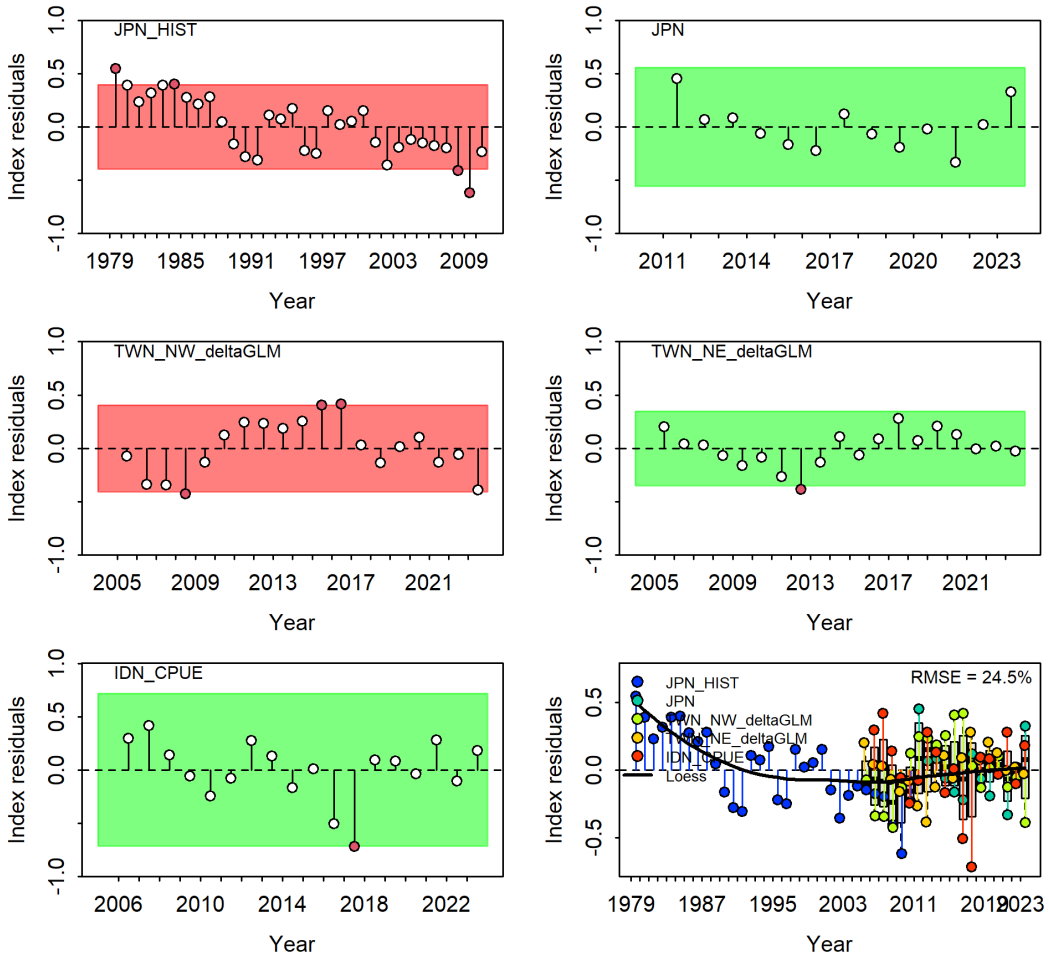

Fig. 9. Runs test plot (green shading indicates no evidence ($p \geq 0.05$) and red shading evidence ($p < 0.05$) to reject the hypothesis of a randomly distributed time-series of residuals, respectively) and Joint residual plot for fits to CPUE indices (vertical lines with points show the residuals, and solid black lines show loess smoother through all residuals, boxplots indicate the median and quantiles in cases where residuals from the multiple indices are available for any given year and root mean squared errors (RMSE) are included in the upper right-hand corner of each plot).

Scenario “S1”

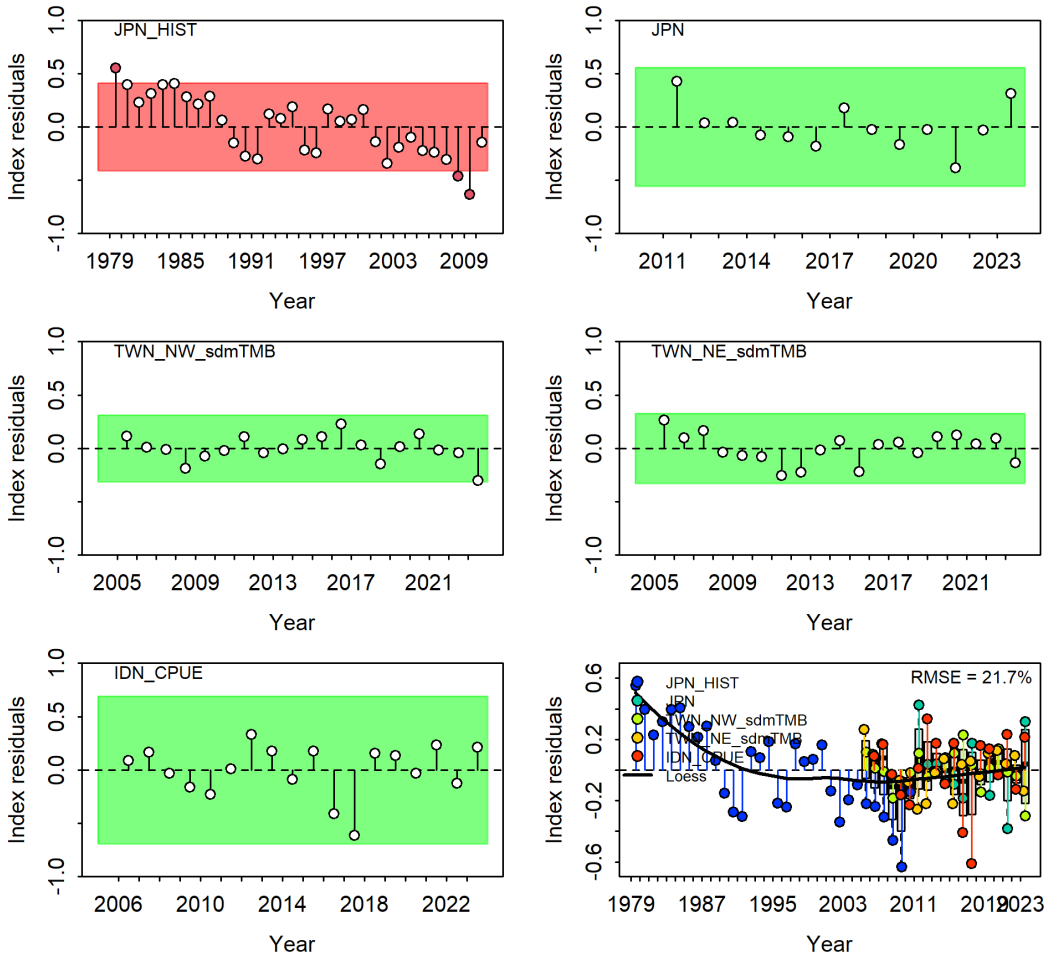

Fig. 9. (continued).

Scenario “S2”

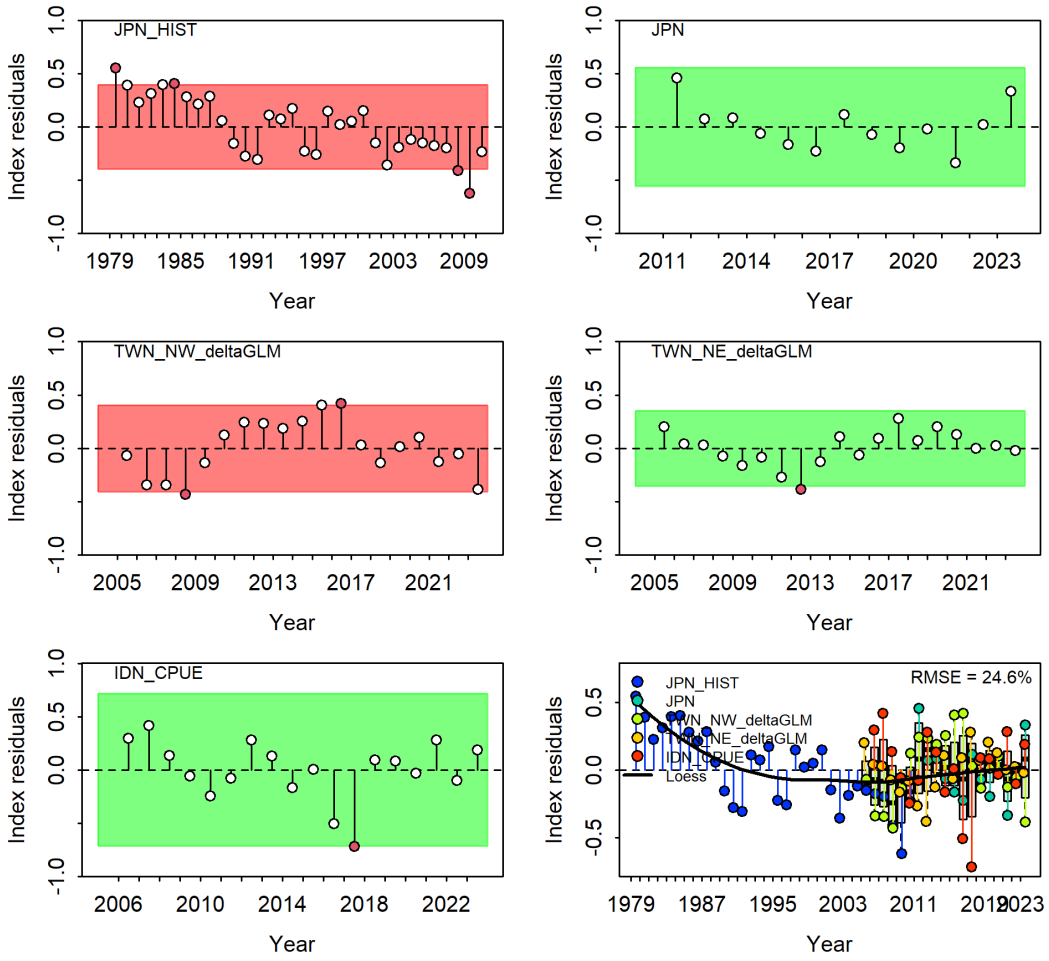

Fig. 9. (continued).

Scenario “S3”

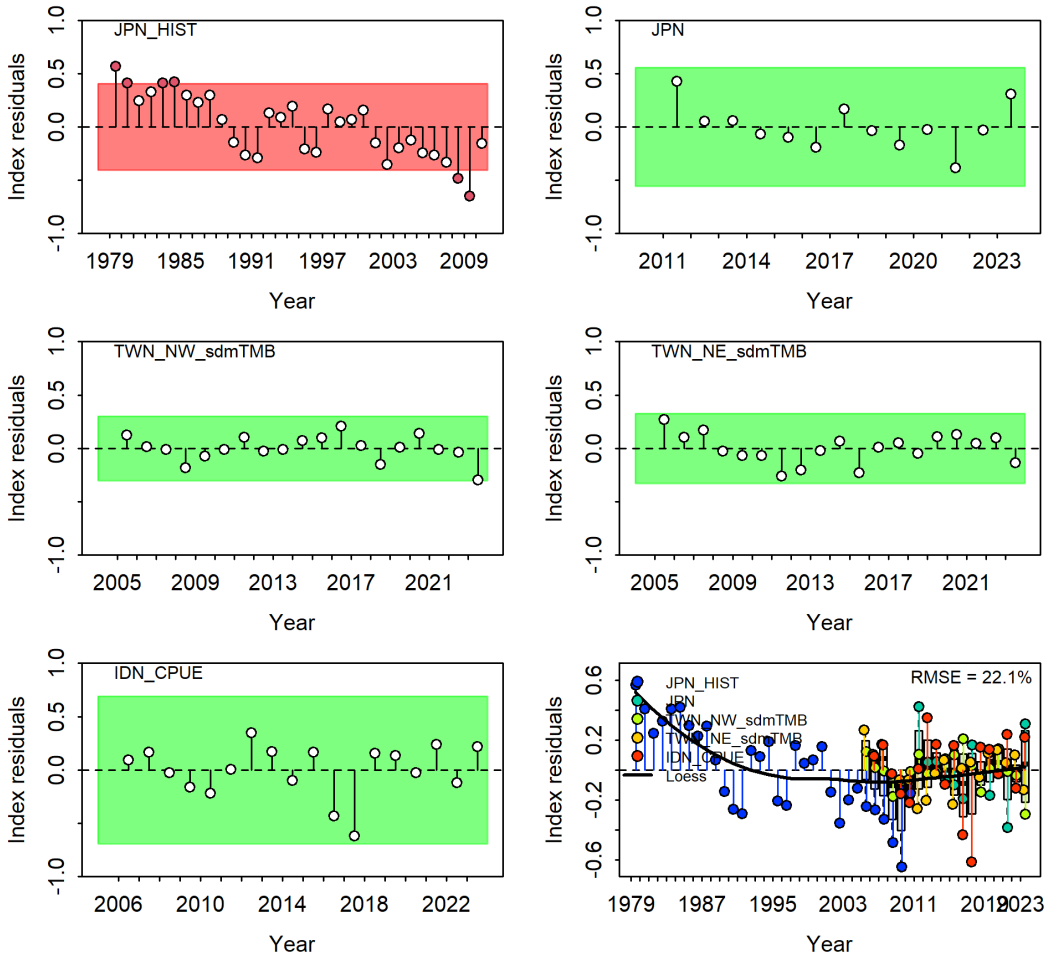

Fig. 9. (continued).

Scenario “S4”

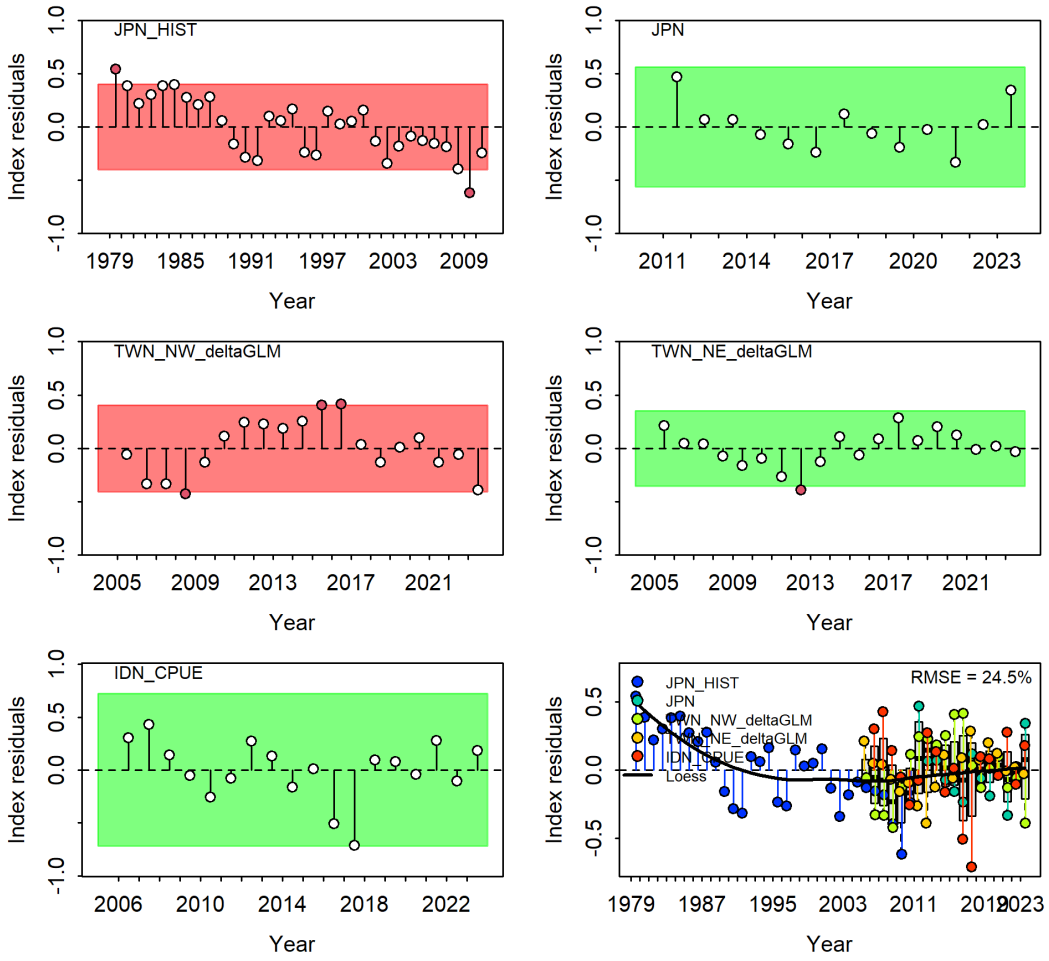

Fig. 9. (continued).

Scenario “S5”

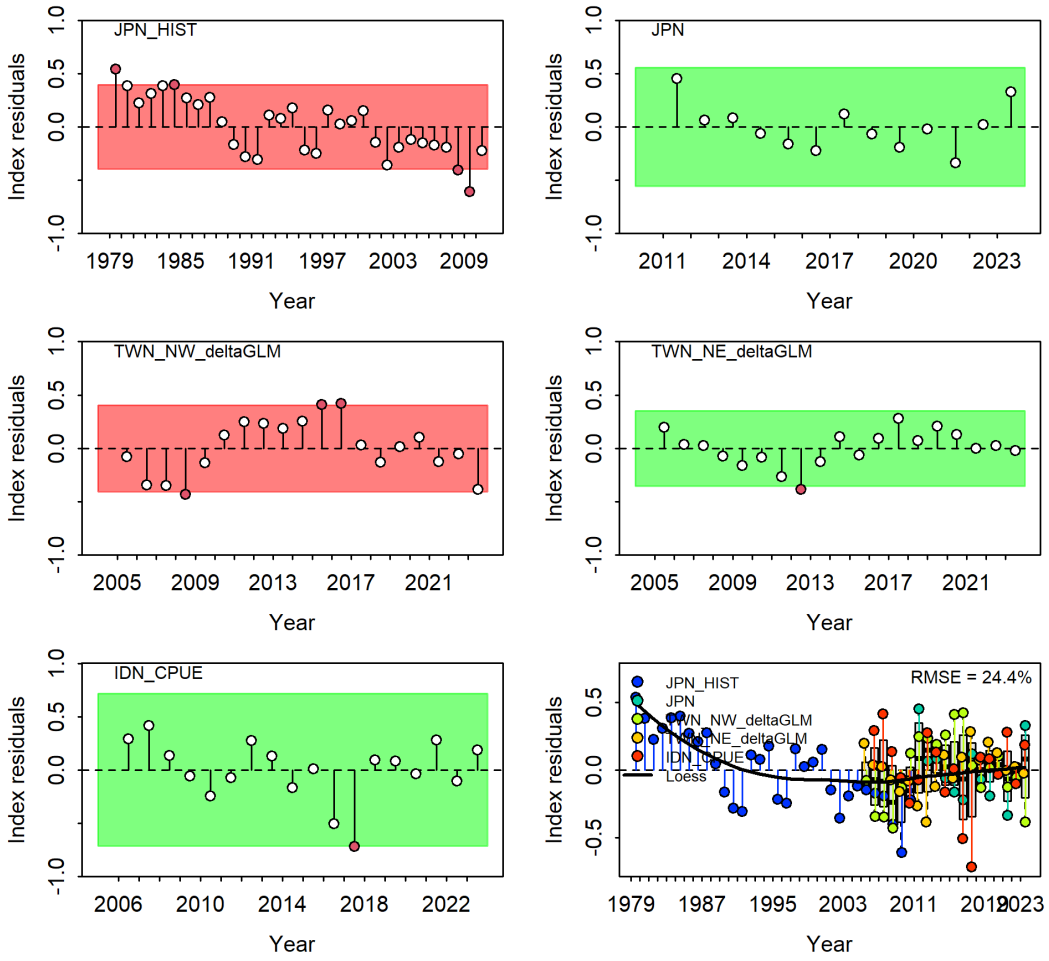

Fig. 9. (continued).

Scenario “S6”

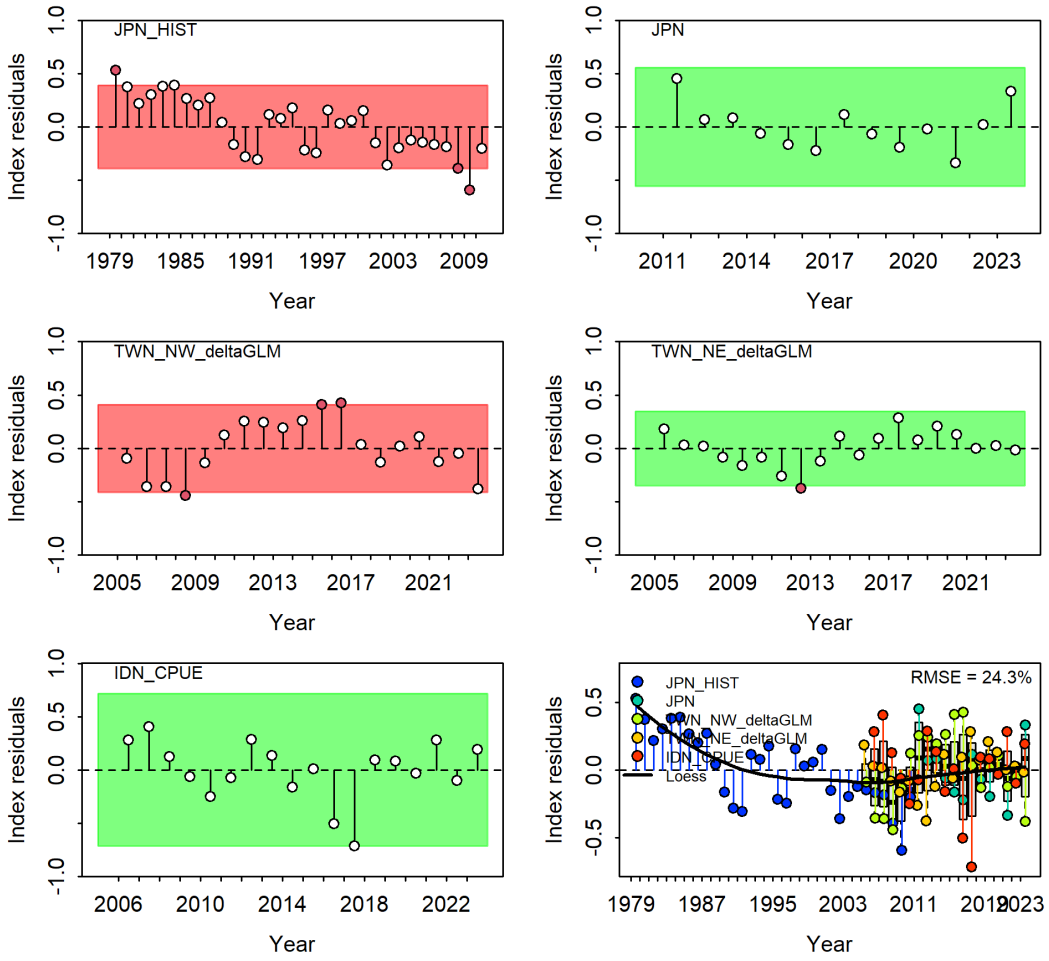

Fig. 9. (continued).

Scenario “S7”

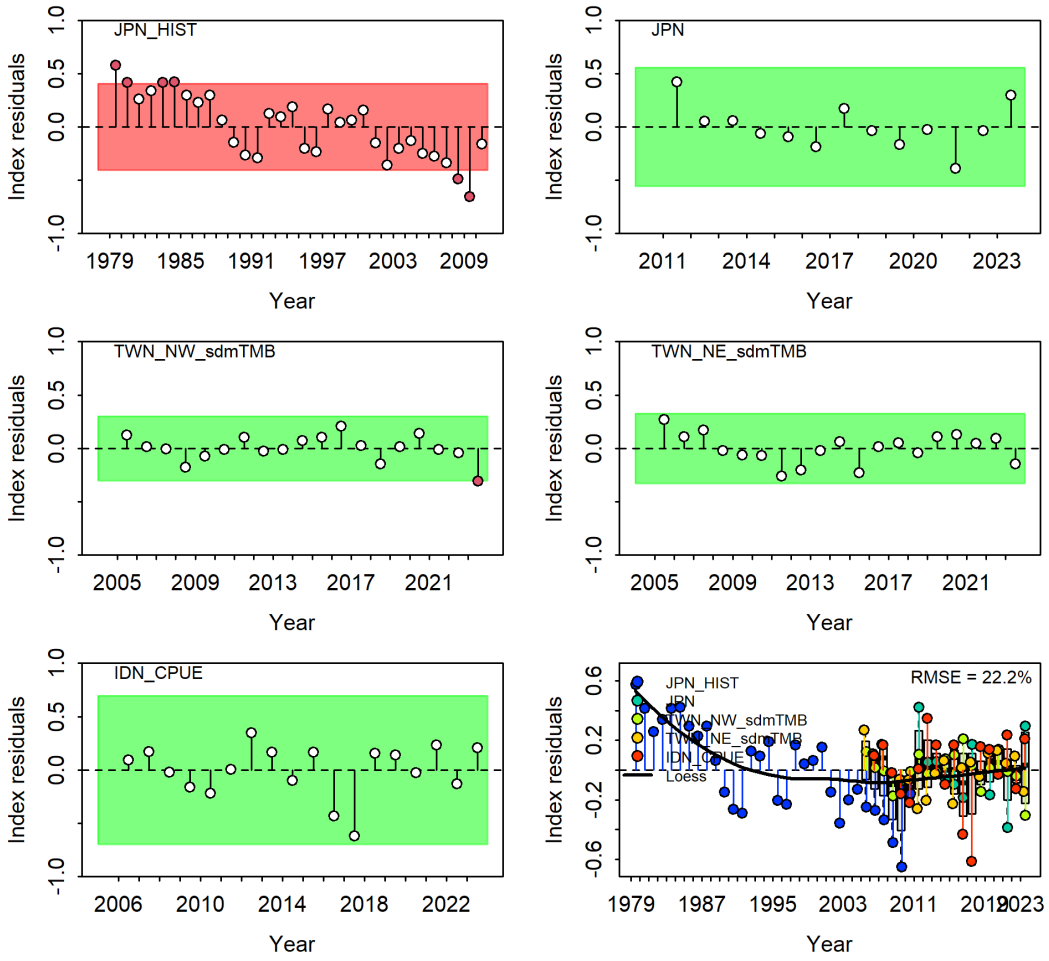

Fig. 9. (continued).

Scenario “S8”

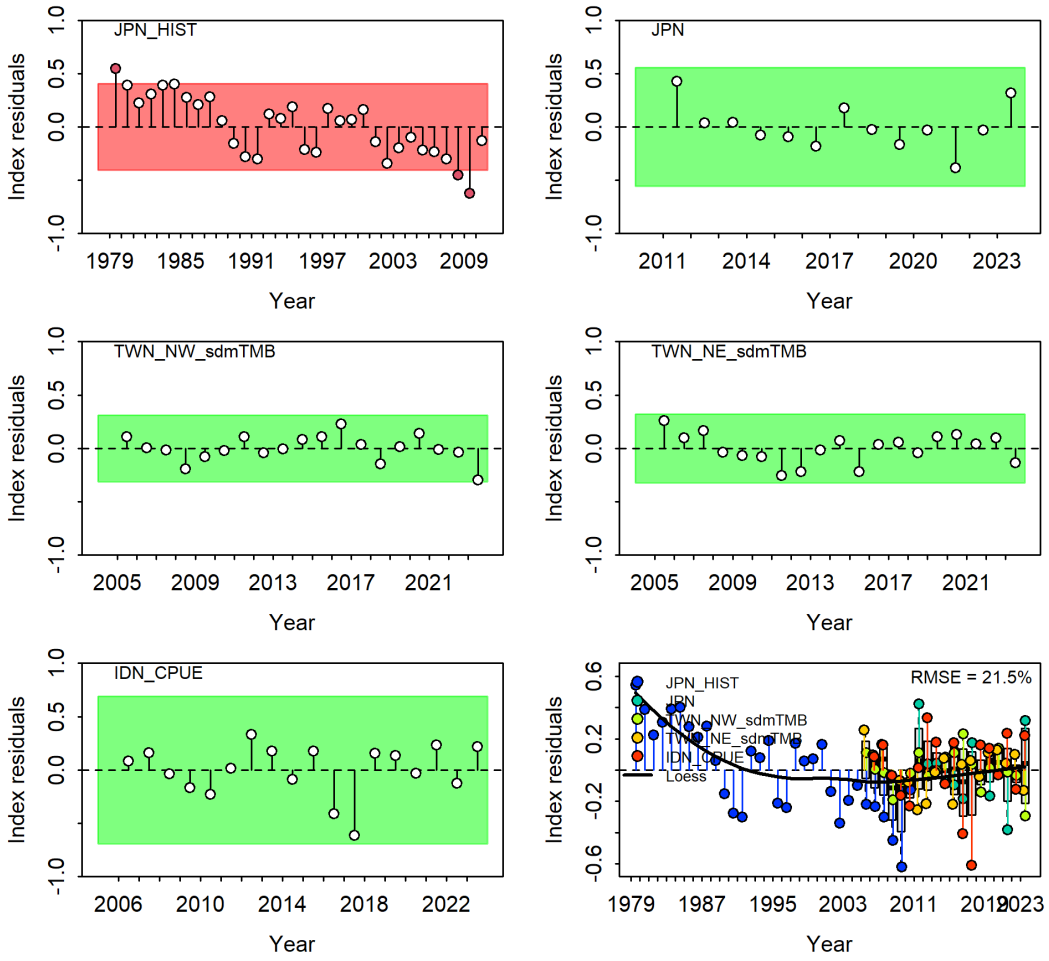

Fig. 9. (continued).

Scenario “S9”

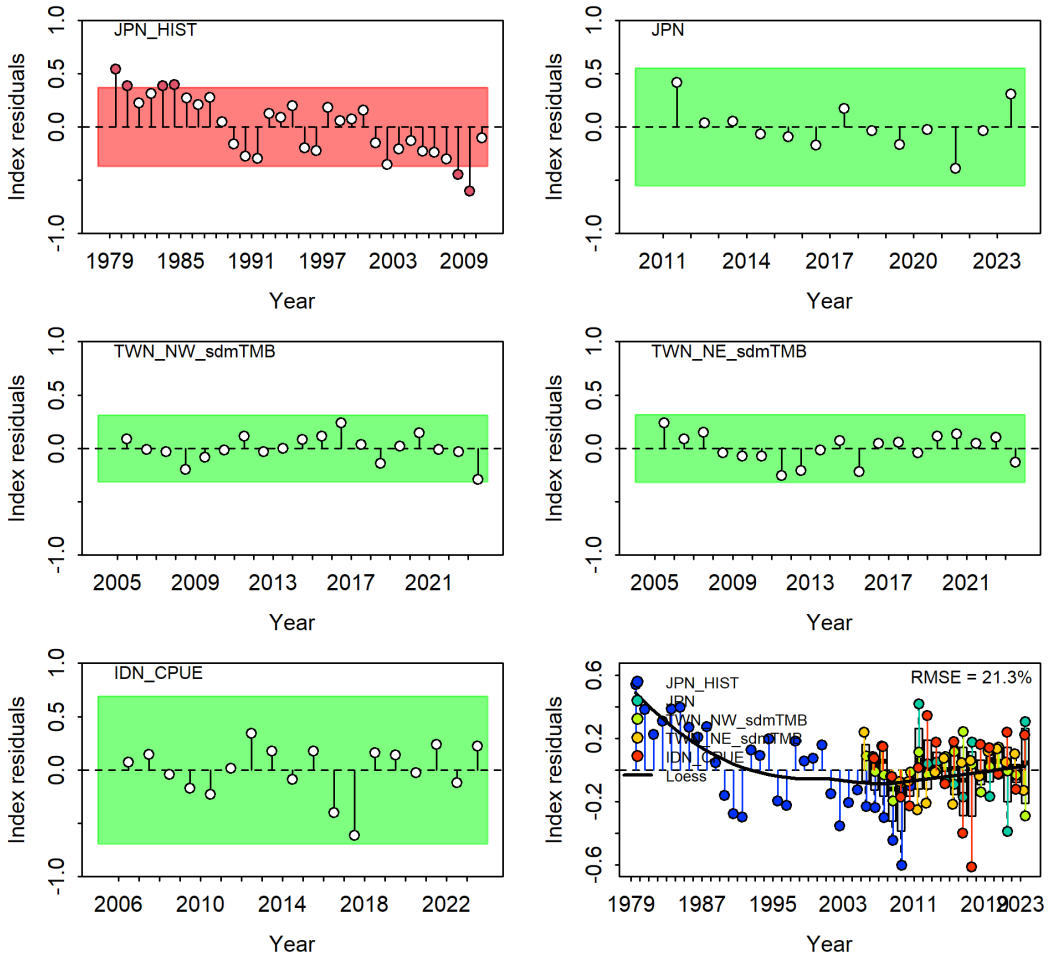

Fig. 9. (continued).

Scenario “S0”

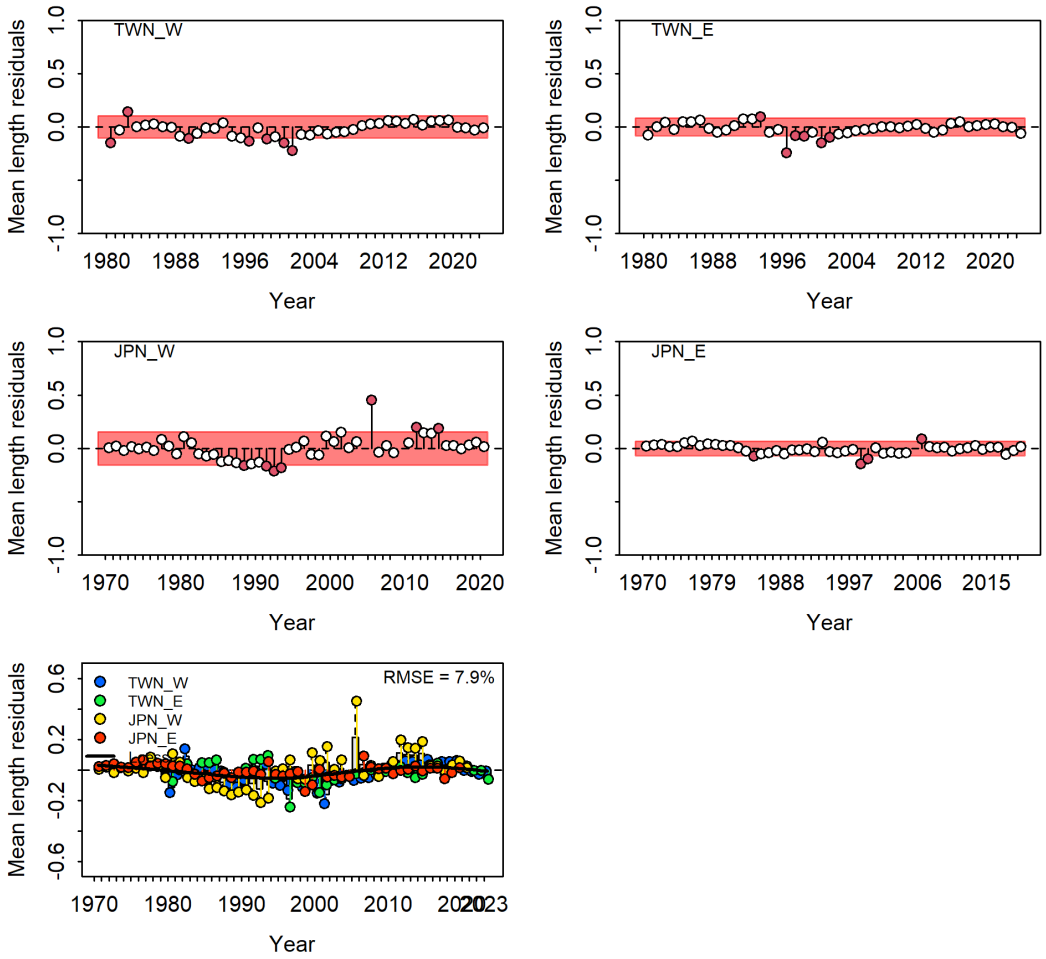

Fig. 10. Runs test plot (green shading indicates no evidence ($p \geq 0.05$) and red shading evidence ($p < 0.05$) to reject the hypothesis of a randomly distributed time-series of residuals, respectively) and joint residual plot for fits to length-frequency data (vertical lines with points show the residuals, and solid black lines show loess smoother through all residuals, boxplots indicate the median and quantiles in cases where residuals from the multiple indices are available for any given year and root mean squared errors (RMSE) are included in the upper right-hand corner of each plot).

Scenario “S1”

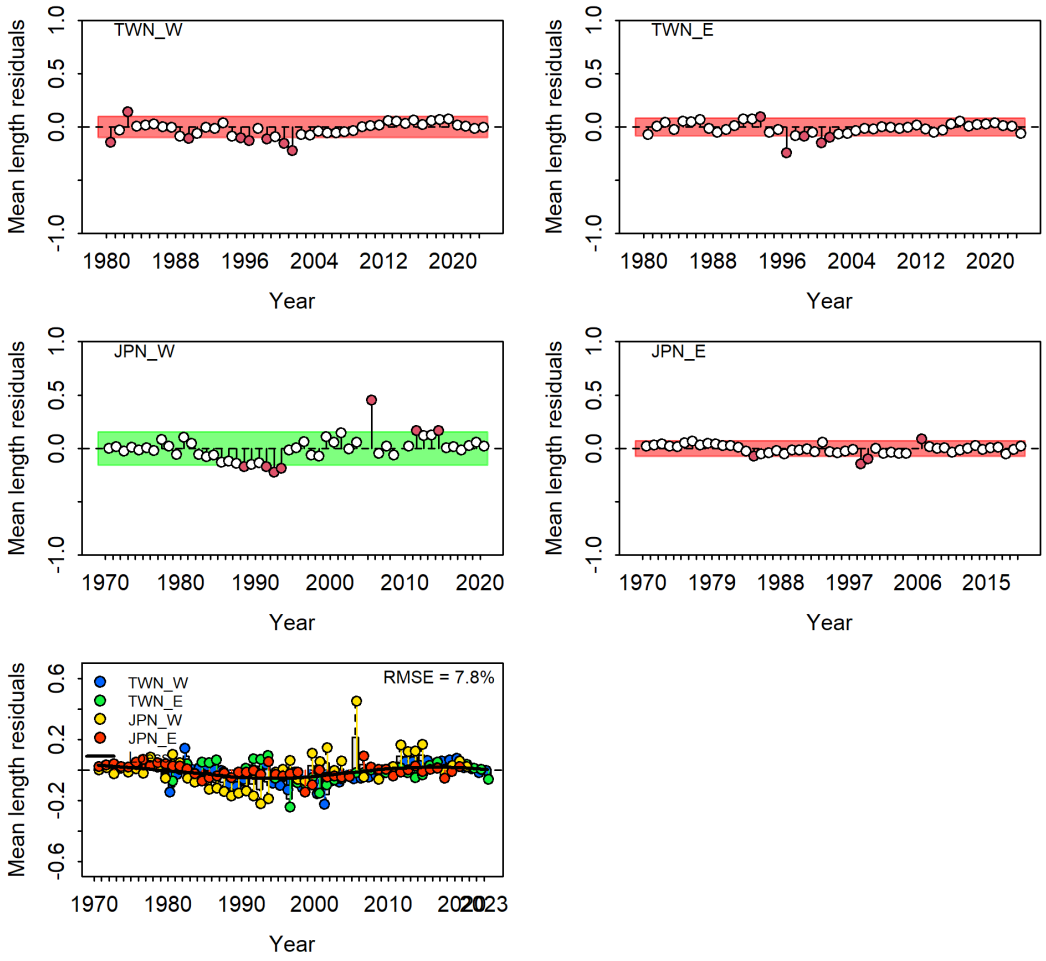

Fig. 10. (continued).

Scenario “S2”

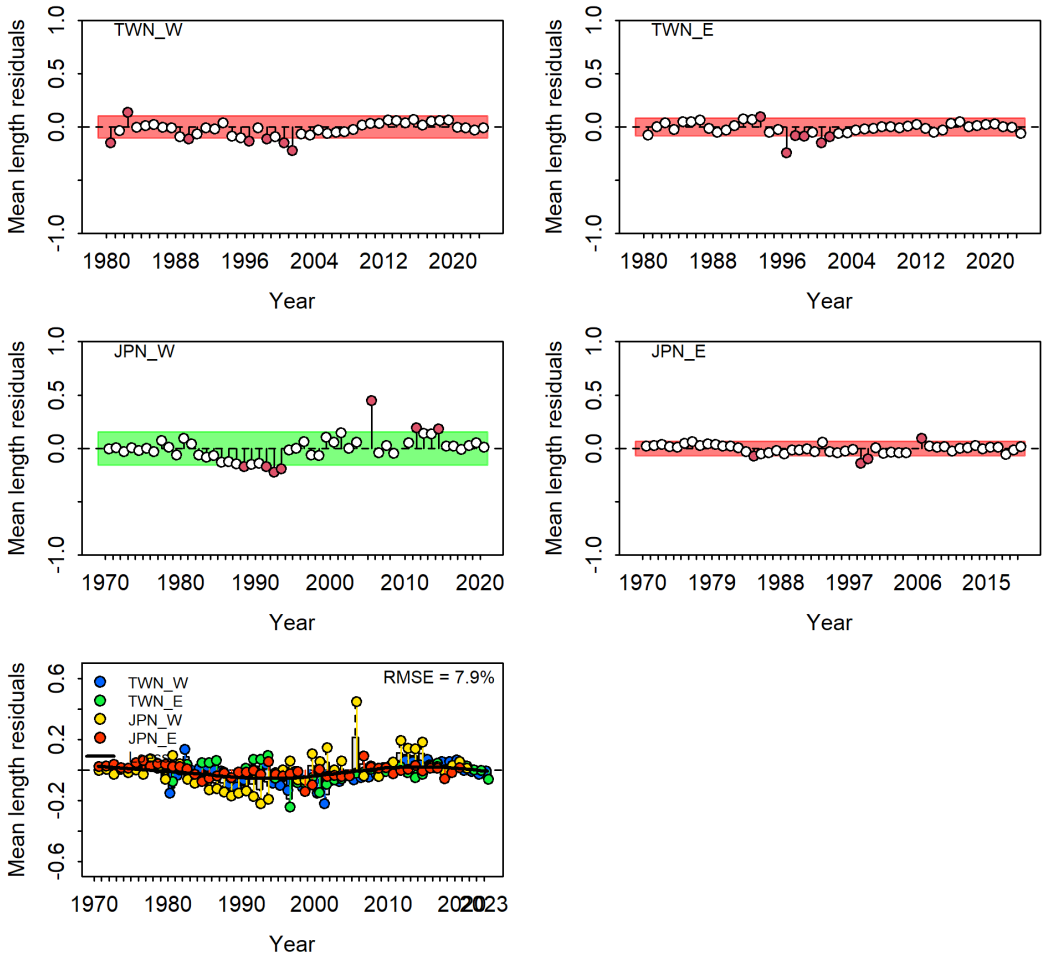

Fig. 10. (continued).

Scenario “S3”

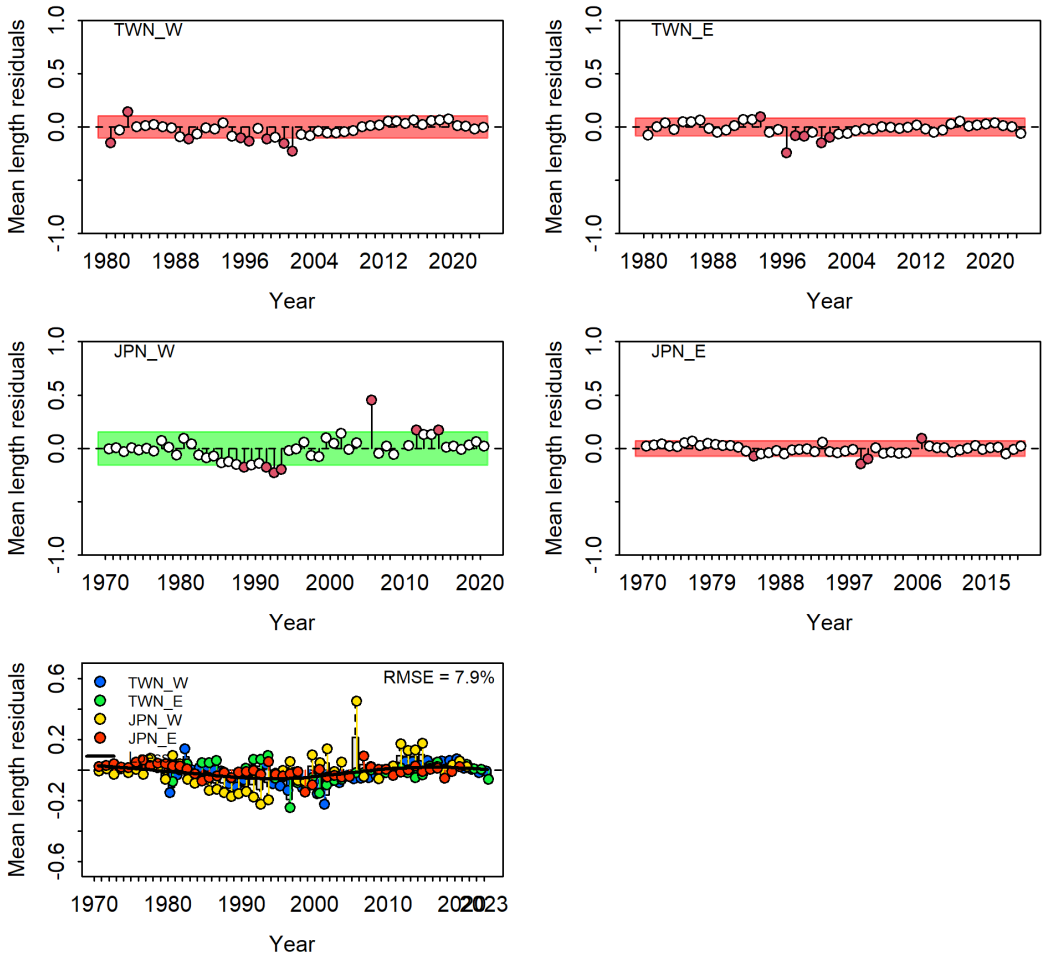

Fig. 10. (continued).

Scenario “S4”

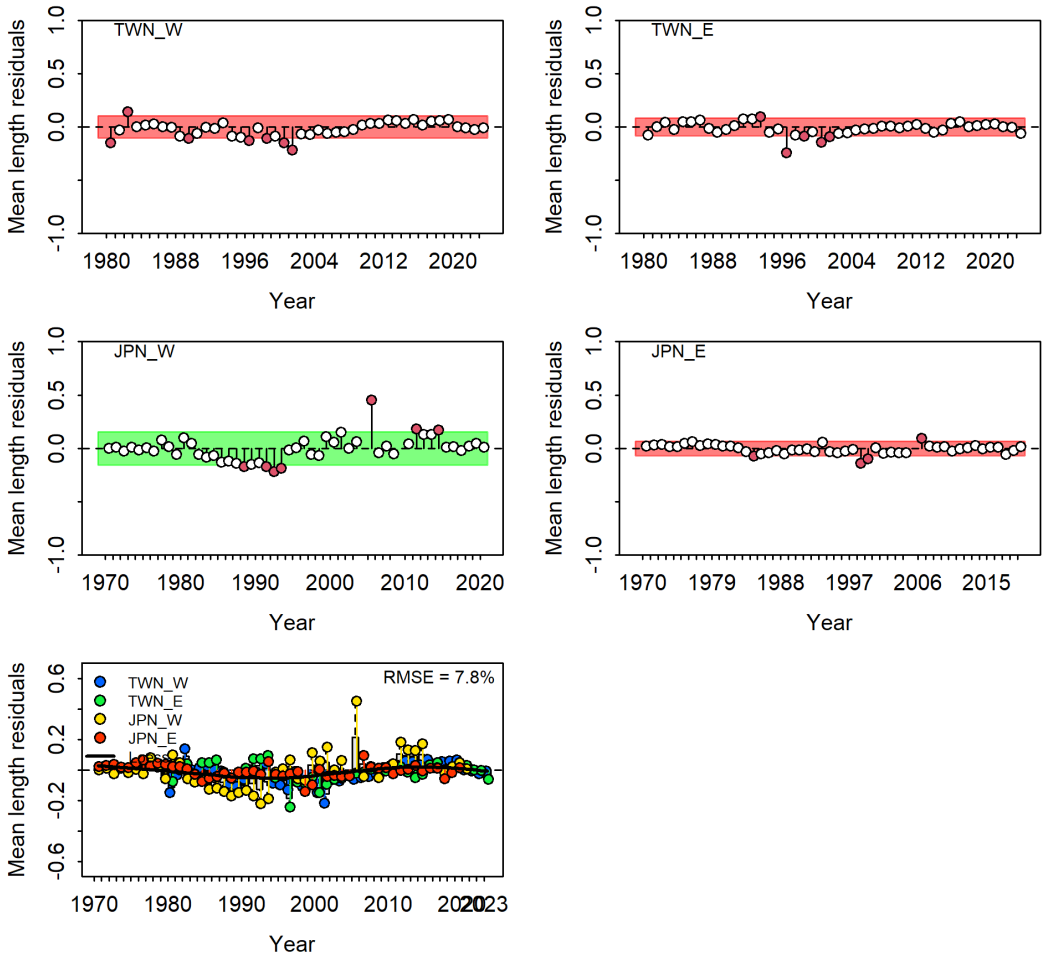

Fig. 10. (continued).

Scenario “S5”

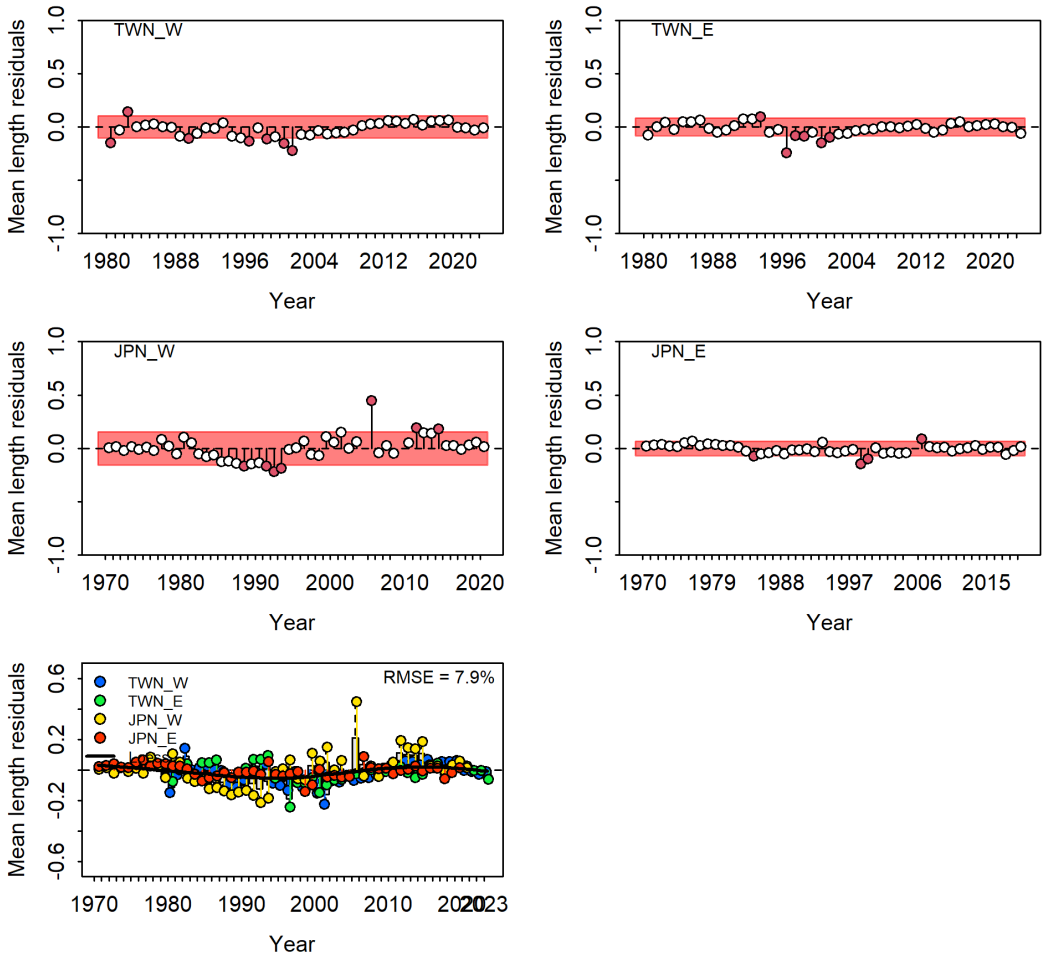

Fig. 10. (continued).

Scenario “S6”

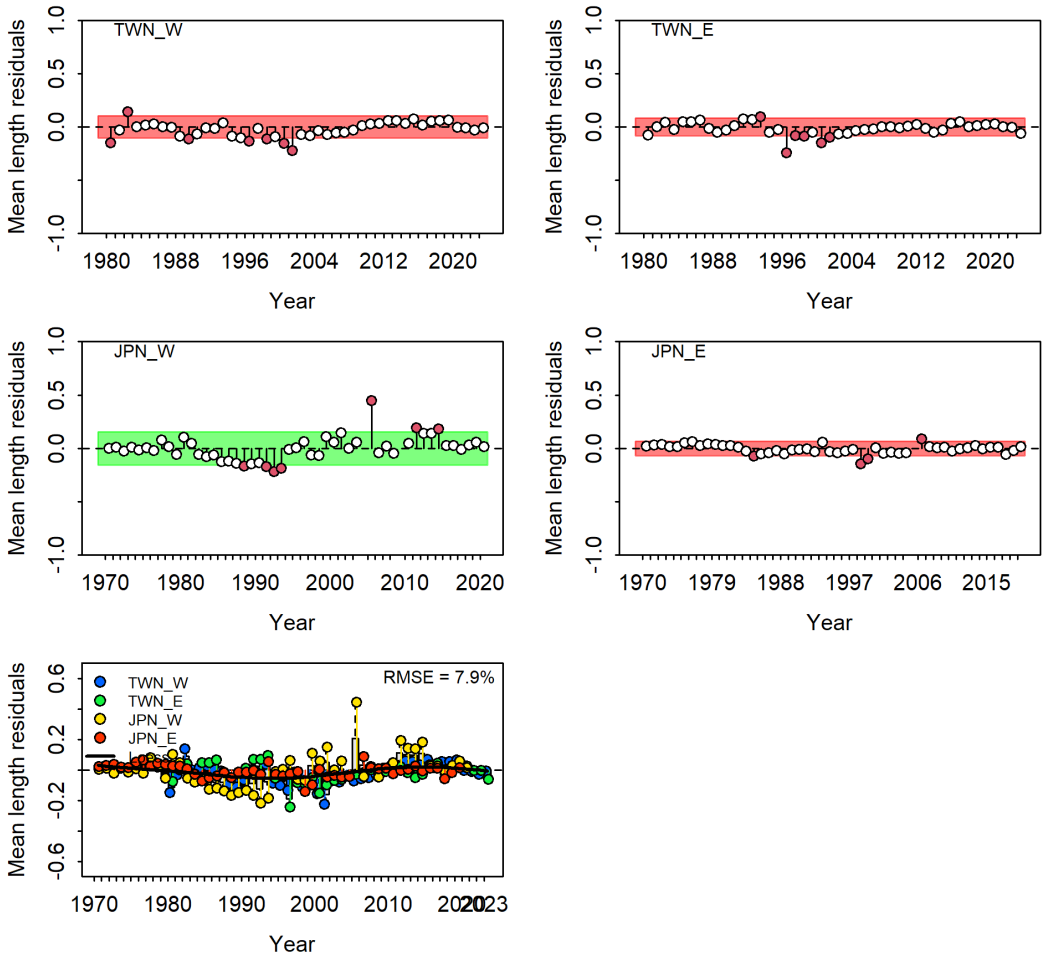

Fig. 10. (continued).

Scenario “S7”

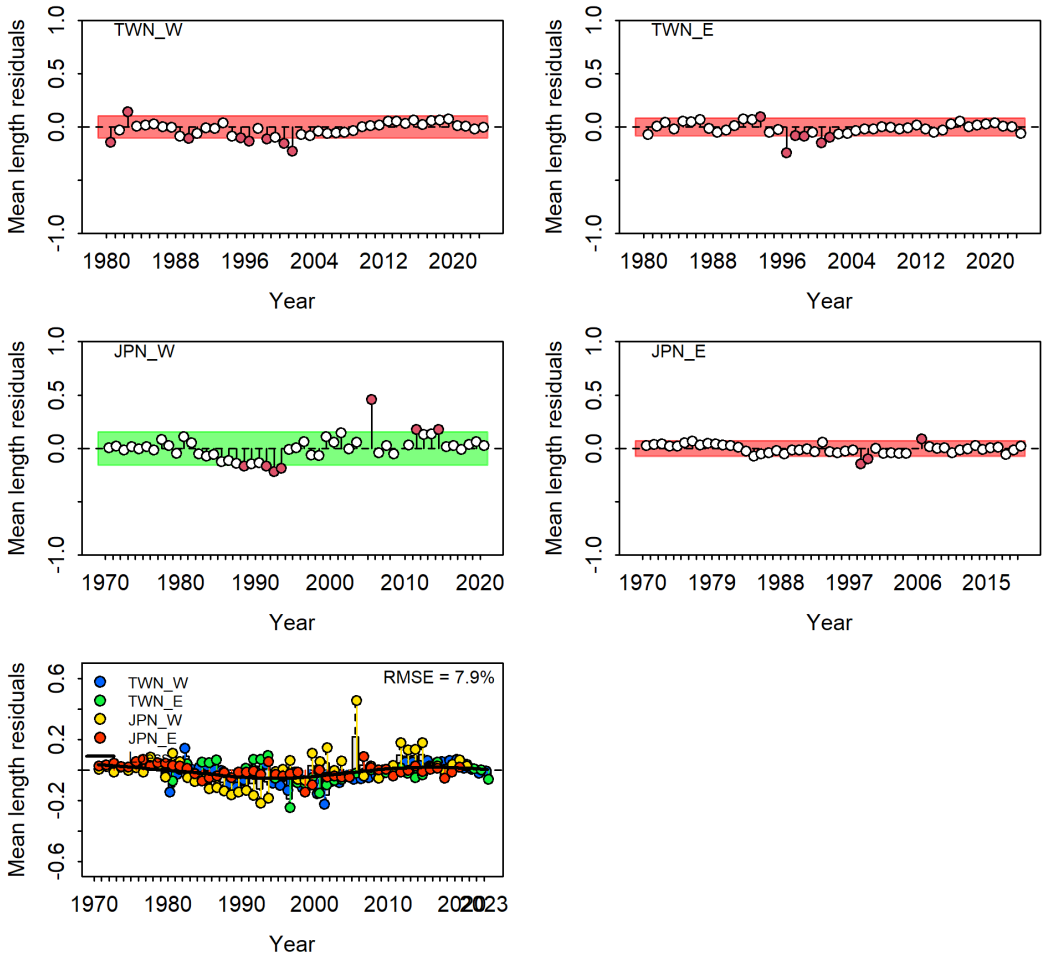

Fig. 10. (continued).

Scenario “S8”

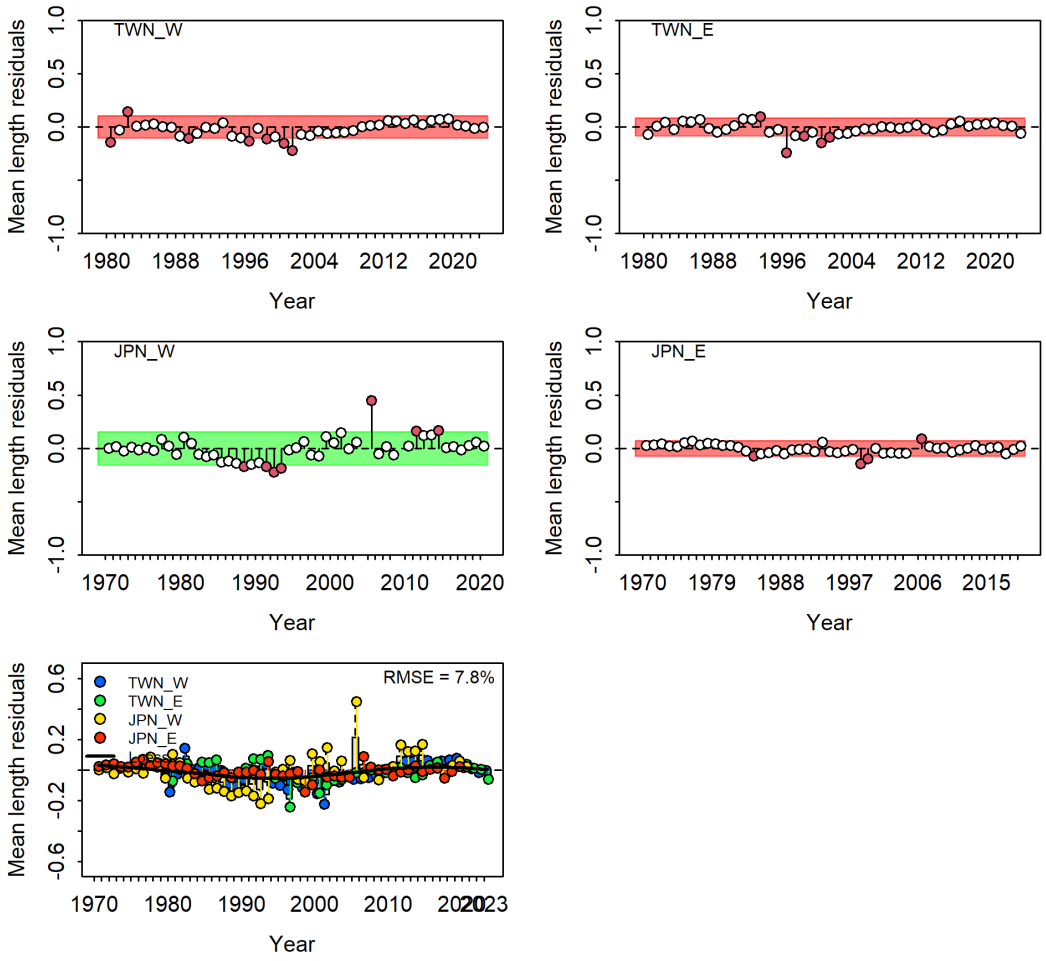

Fig. 10. (continued).

Scenario “S9”

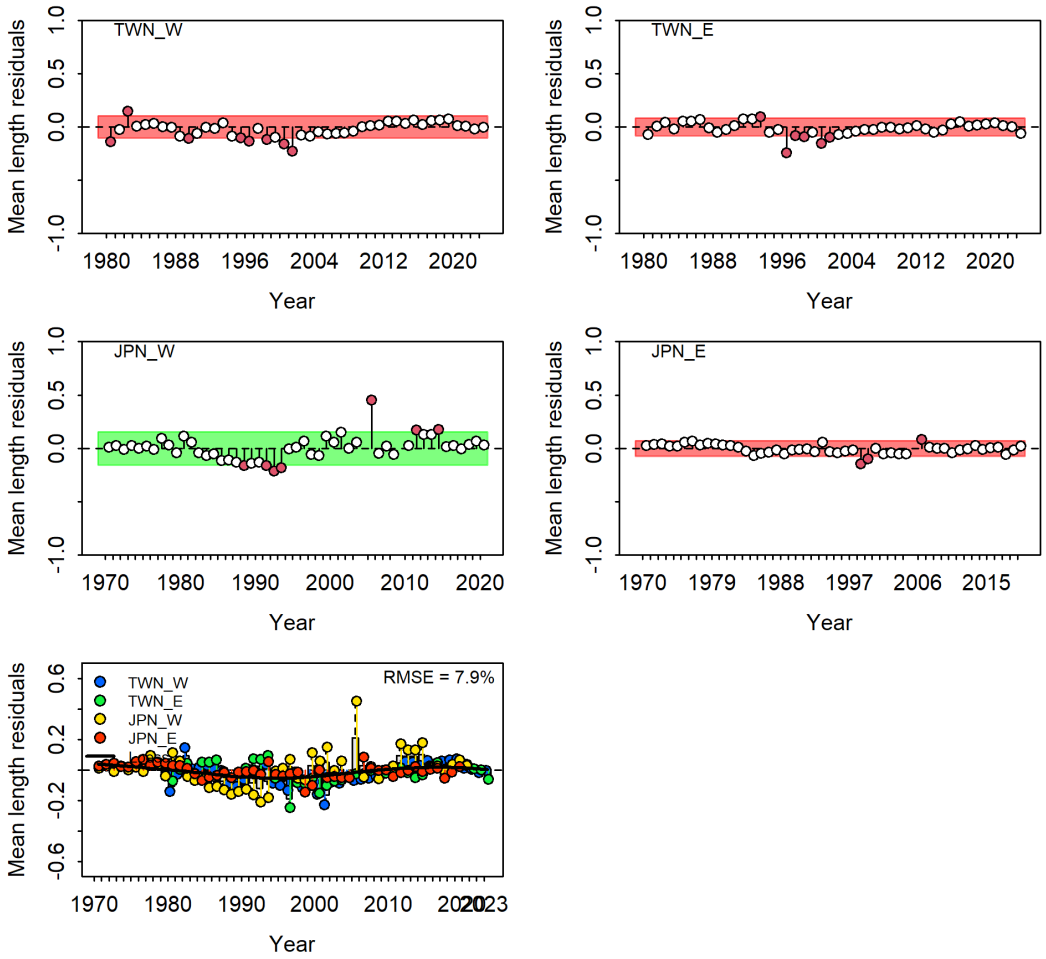

Fig. 10. (continued).

Two-area scenarios

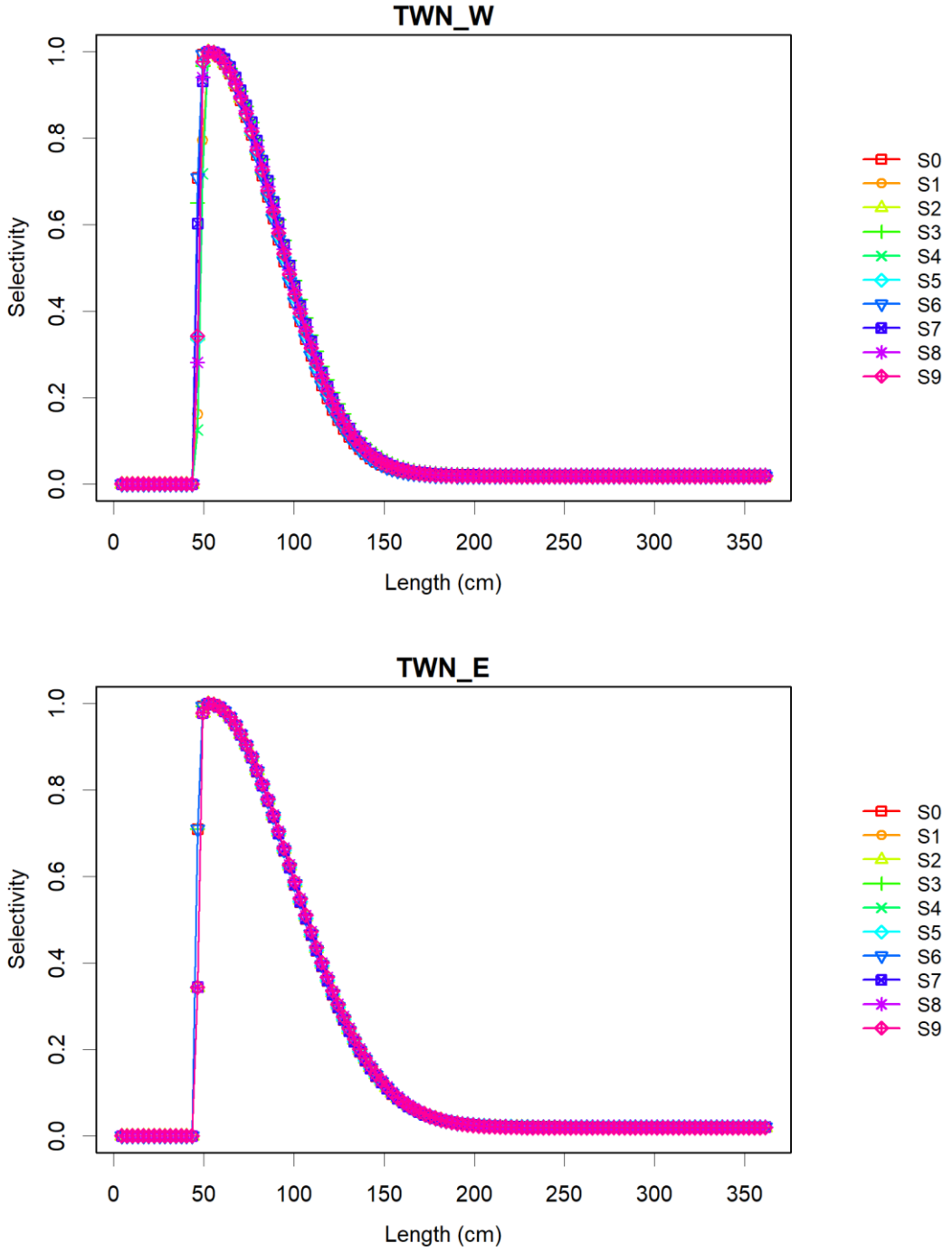

Fig. 11. Model-estimated selectivity for blue marlin in the Indian Ocean.

Two-area scenarios

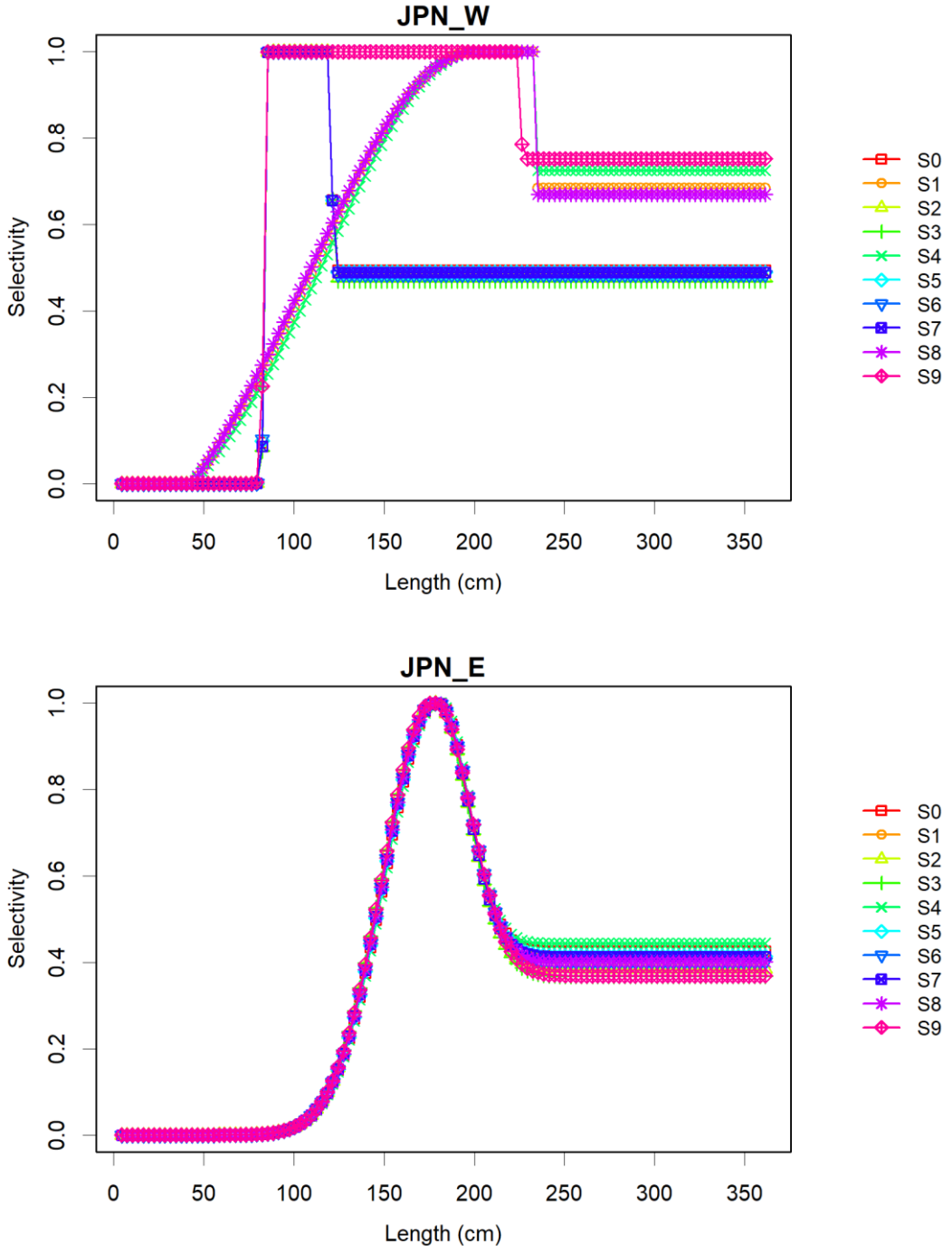

Fig. 11. (continued).

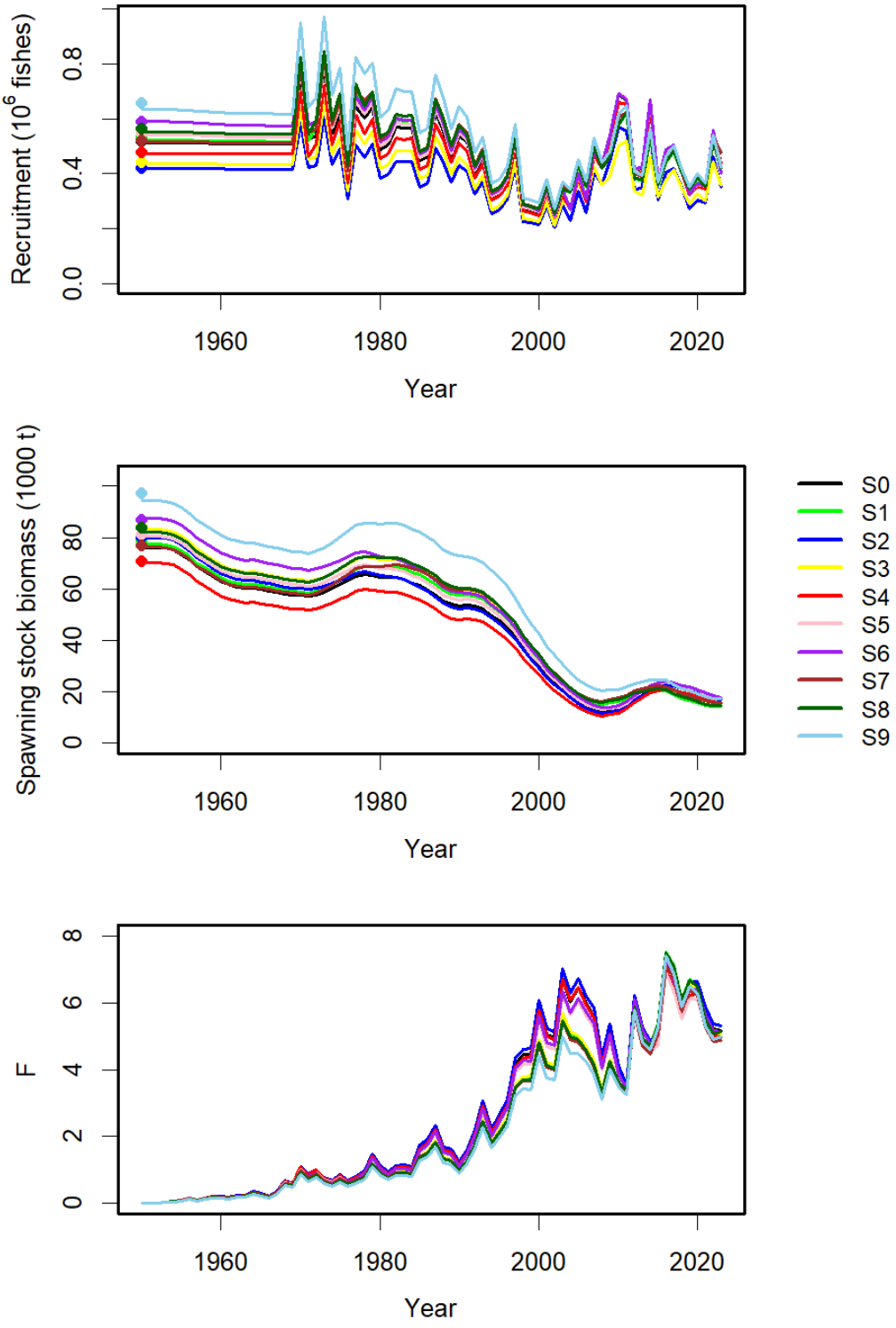

Fig. 12. Time trajectories of the model-estimated recruitment, spawning biomass and fishing mortality of blue marlin in the Indian Ocean.

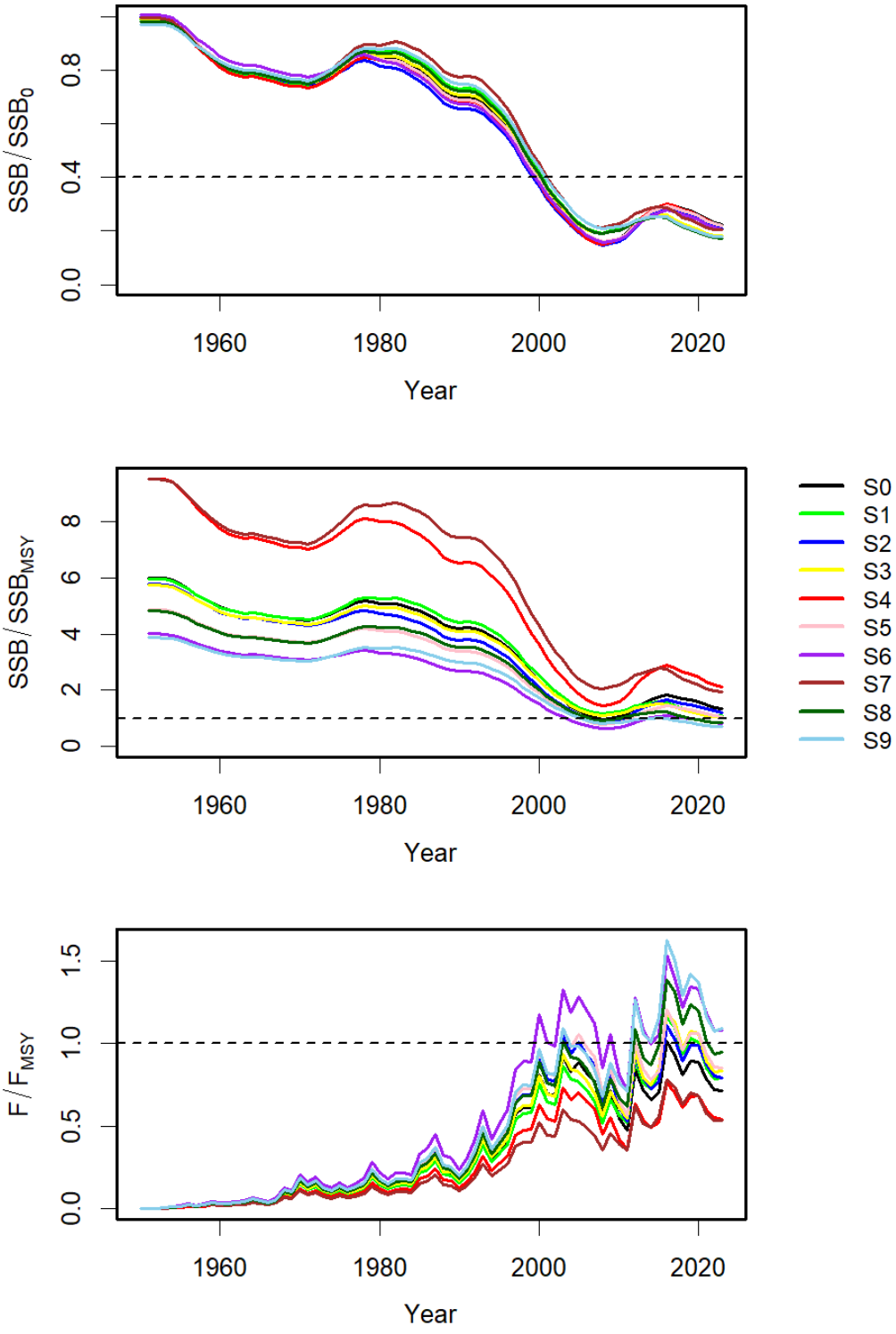

Fig. 13. Time trajectory of the model-estimated relative fishing mortality and spawning biomass of blue marlin in the Indian Ocean.

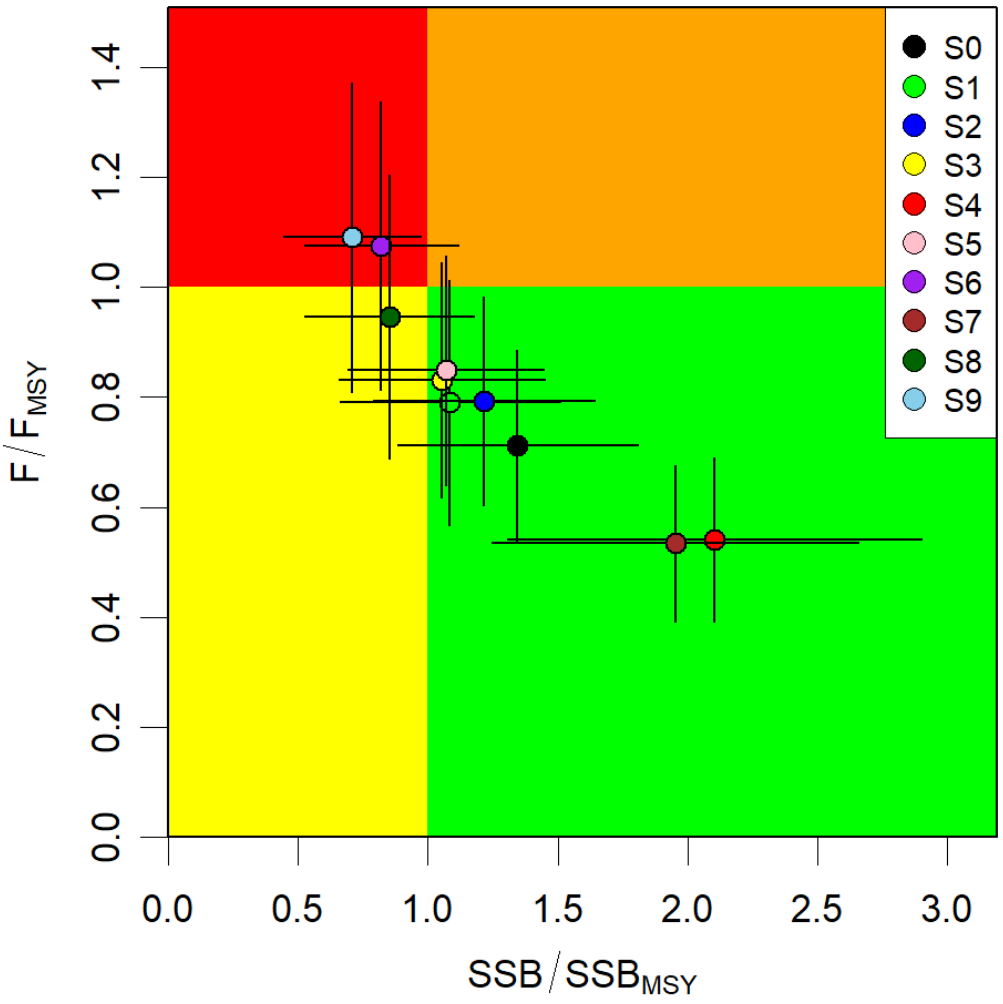

Fig. 14. Kobe plot for blue marlin in the Indian Ocean.

Scenario (S0)

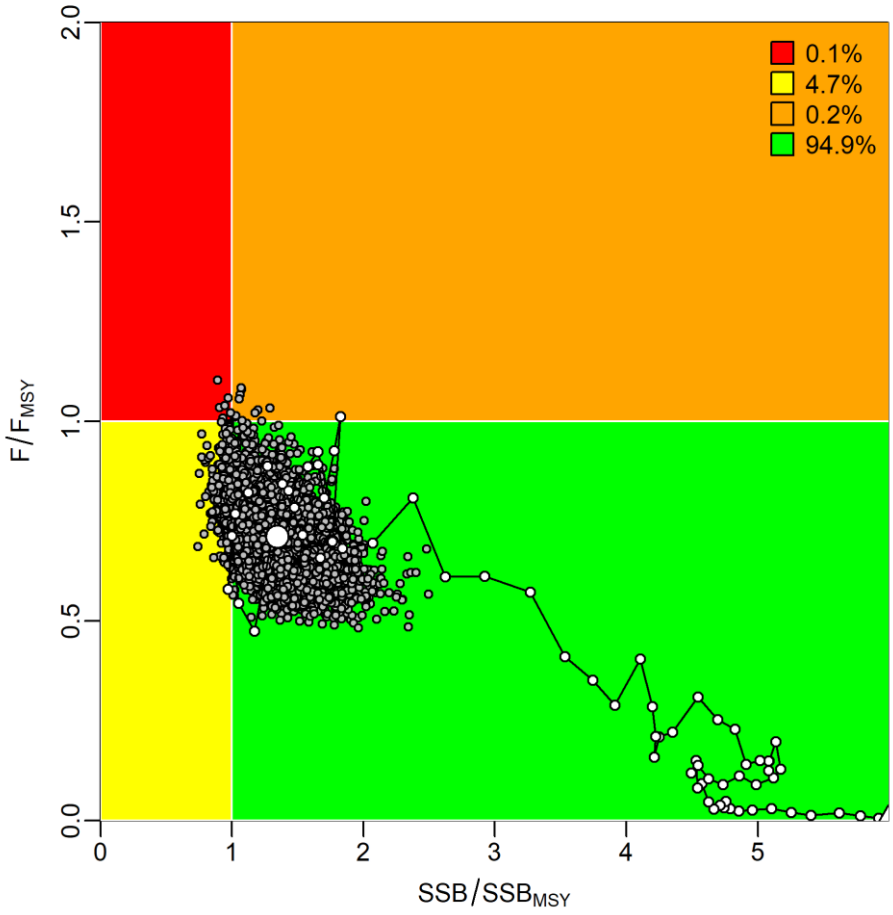

Fig. 15. Kobe plot for blue marlin in the Indian Ocean obtained from selected scenario (S0).

Scenario (S1)

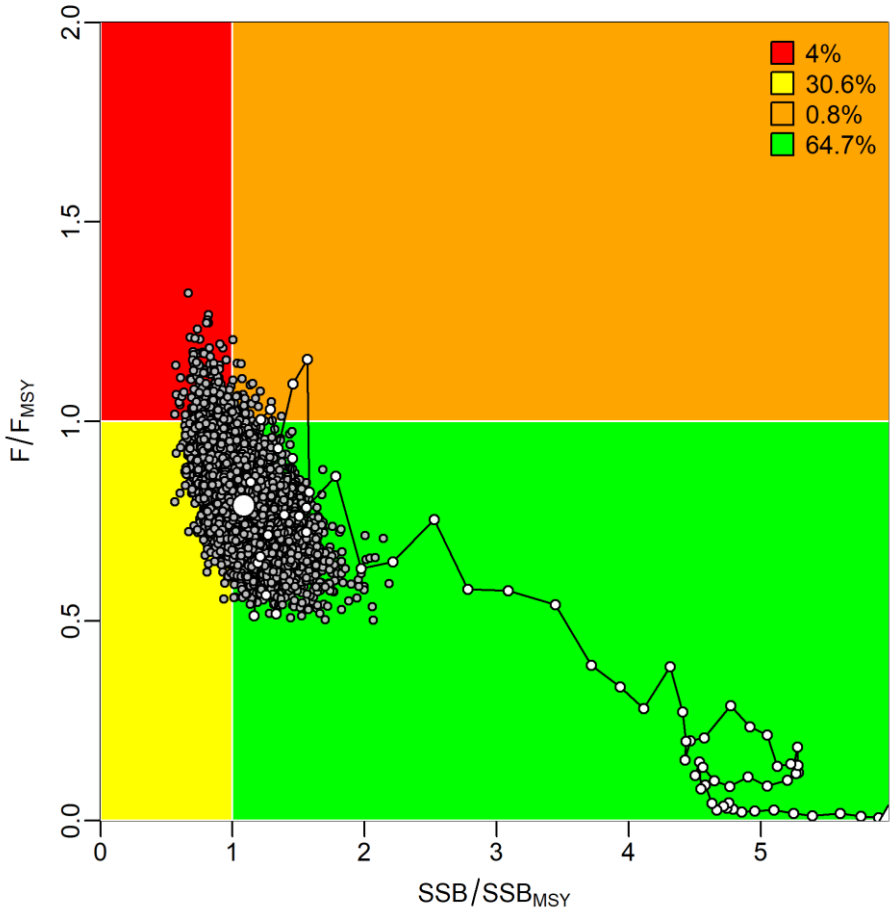

Fig. 15. (continued).

Table 1. Life-history parameters of blue marlin used in this study.

Parameter	Female	Male
Natural mortality (M, year^{-1})	0.22	0.37
Length at youngest age ($L1$, cm)	144.000	144.000
Length at oldest age ($L2$, cm)	304.178	226.000
Growth coefficient (K, year^{-1})	0.107	0.211
Length-Weight (a)	1.844E−05	1.37E−05
Length-Weight (b)	2.956	2.975
Length at 50% maturity (cm)	179.76	
Maturity slope	-0.25	
Spawner-recruit steepness (h)	0.87	0.87
Variation in recruitment (σ)	0.4	0.4

Table 2. Model assumptions of scenarios conducted for sensitivity analysis.

Scenario	Fleet	CPUE used	Natural Mortality	Steepness (h)
S0	TWN_W, TWN_E, JPN_W, JPN_E, IDN, OTH_W and OTH_E	JPN_HIST (1979-2010), JPN (2011-2023), TWN_NW_deltaGLM, TWN_NE_deltaGLM, IDN ("S10" of the previous assessment in 2022)	Age-specific mortalities were scaled	0.87
S1	Same with "S0"	JPN (1979-2010), JPN (2011-2023), TWN_NW_sdmTMB, TWN_NE_sdmTMB, IDN	Age-specific mortalities were scaled	0.87
S2	Same with "S0"	Same with "S0"	Fixed	0.87
S3	Same with "S0"	Same with "S1"	Fixed	0.87
S4	Same with "S0"	Same with "S0"	Age-specific mortalities were scaled	0.95
S5	Same with "S0"	Same with "S0"	Age-specific mortalities were scaled	0.8
S6	Same with "S0"	Same with "S0"	Age-specific mortalities were scaled	0.7
S7	Same with "S0"	Same with "S1"	Age-specific mortalities were scaled	0.95
S8	Same with "S0"	Same with "S1	Age-specific mortalities were scaled	0.8
S9	Same with "S0"	Same with "S1	Age-specific mortalities were scaled	0.7

Table 3. The estimates of key management quantities for blue marlin in the Indian Ocean.

Scenario	R_0	SSB_0	MSY	F_{MSY}	SSB_{MSY}	SSB_{2023}/SSB_0	SSB_{2023}/SSB_{MSY}	F_{2023}/F_{MSY}
S0	517.45	76,651	8,845	7.276	12,706	0.223	1.346	0.711
S1	530.589	78,598	9,070	6.509	13,000	0.180	1.086	0.790
S2	420.888	79,967	8,270	6.702	13,843	0.211	1.217	0.793
S3	442.391	84,053	8,681	6.094	14,510	0.182	1.054	0.831
S4	476.091	70,525	9,547	9.195	7,377	0.220	2.104	0.540
S5	546.253	80,918	8,308	5.751	16,526	0.218	1.070	0.849
S6	586.475	86,876	7,556	4.784	21,818	0.206	0.820	1.076
S7	518.547	76,814	10,367	9.149	8,023	0.204	1.952	0.534
S8	564.177	83,573	8,576	5.418	17,046	0.174	0.851	0.947
S9	655.762	97,140	8,415	4.576	24,367	0.178	0.709	1.091